NUCLEAR SPIN-LATTICE RELAXATION TIMES IN METALS

David Brown

A Thesis Submitted for the Degree of PhD
at the
University of St Andrews

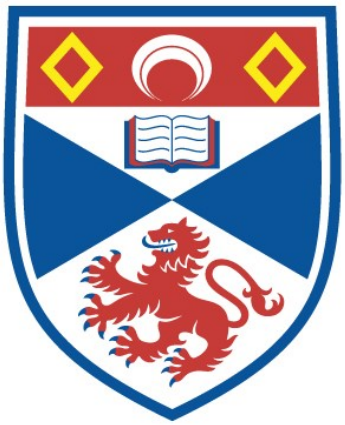

1970

NUCLEAR SPIN-LATTICE RELAXATION TIMES IN METALS

A Thesis

presented by

David Brown, B.Sc.

to the

University of St. Andrews

in application for the Degree

of Doctor of Philosophy.

ProQuest LLC.
789 East Eisenhower Parkway
P.O. Box 1346
Ann Arbor, MI 48106 – 1346

DECLARATION

I hereby certify that this thesis has been composed by me, and is a record of work done by me, and has not previously been presented for a Higher Degree.

This research was carried out in the Physical Science Laboratory of St. Salvator's College, in the University of St. Andrews, under the supervision of Dr. D.P. Tunstall.

(David Brown)

PERIODICAL	PHYSICS LIBRARY
Annales de Physique	
Annals of Physics	Vol. 1, 1957 onw
Annual Review of Nuclear Science	Vol. 1, 1952 onw
Applied Physics Letters	Vol. 1, 1962 onw
Applied Scientific Research	Vol. A1, 1949 on Vol. B1, 1950 on
Arkiv för Fysik	Vol. 1, 1949 onw
Australian Journal of Physics	Vol. 1, 1948 onw
Bell System Technical Journal	Vol. 24, 1945 on
British Journal of Applied Physics	Vol. 1, 1950 onw
Bulletin Ampere	
Bulletin of the Institute of Physics & the Physical Society	Vol. 7, 1956 onw
Bulletin of the Polish Academy of Sciences	Vol. 1, 1953 onw

No of Si^{29} nuclei/cm^3 = $\frac{6.0\times10^{23}\ 2.3}{29}\times 0.047$ — $\frac{gm}{gm}$ $\frac{}{cm^3}$

$\frac{4}{3}\pi R^3 N =$

$N_{Si} = 2.1\times10^{21}\ cm^{-3}$

∴ Av spacing of Si^{29} nuclei $\sim \left(\frac{3}{4\pi N_{Si}}\right)^{1/3} \sim 4.8\ 10^{-8}$ cm

$\sim 4\ 10^{-10}$

Interatomic spacing ca $5.5\cdot10^{-8}$ cm. no of Si atoms/cm^3 $\frac{3.7}{4\pi R^3}\sim 1.4$

Now 4.7% contain Si^{29} so no. of Si^{29} atoms/cm^3 is $6.5\ 10^{19}$ (1.75

∴ Av spacing of Si^{29} nuclei is $\sim \left(\frac{3}{4\pi\ 6.5\times10^{19}}\right)^{1/3}$ $\sim 1.5\ 10^{-7}$ cm. (1.1

$\sim 15\ 10^{-8}$ cm $\sim 3a$

$B_{dip} \sim \frac{\mu}{4\pi}\frac{\mu_{Si}}{9a^3}$ $\qquad \mu_{Si} \sim 0.55\times 5.1\ 10^{-27}$ J.T^{-1}

$\sim \frac{10^{-7}\ 0.55\cdot 5.1\ 10^{-27}}{9\ (5.5)^3\ 10^{-30}} \sim 1.9\ 10^{-3}\ \frac{10^{+34}}{10^{34}}$

$B_{dip} \sim \frac{\mu_0}{4\pi}\frac{0.55\cdot 5.1\ 10^{27}}{9.64\ 10^{-30}}$

$\sim 4.9\ 10^{-3}$ G.

perhaps ~ 0.01 G.

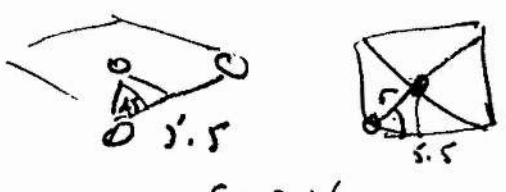

r = 2.4/cos 45

= 4

CERTIFICATE

I certify that David Brown, B.Sc., has spent nine terms at research work in the Physical Science Laboratory of St. Salvator's College, in the University of St. Andrews, under my direction, that he has fulfilled the conditions of Ordinance No. 16 (St. Andrews) and that he is qualified to submit the accompanying thesis in application for the Degree of Doctor of Philosophy.

_____

Research Supervisor

CAREER

I first matriculated in the University of St. Andrews in October 1962. I studied Mathematics and Natural Philosophy, and obtained First Class Honours in Natural Philosophy in 1966.

In October 1966, following the award of an S.R.C. Research Studentship, I was enrolled as a research student under Ordinance 12, and was transferred to Ordinance 16 in October 1967 as a candidate for the degree of Ph.D.

ACKNOWLEDGEMENTS

The author wishes to express his sincere thanks to Dr. D.P. Tunstall for his patient guidance throughcut this research and his stimulating discussions which greatly enhanced the author's understanding, and to Professor J.F. Allen, F.R.S. for providing the excellent facilities and funds. He is also indebted to Mr. J. Watson for his invaluable assistance in technical matters.

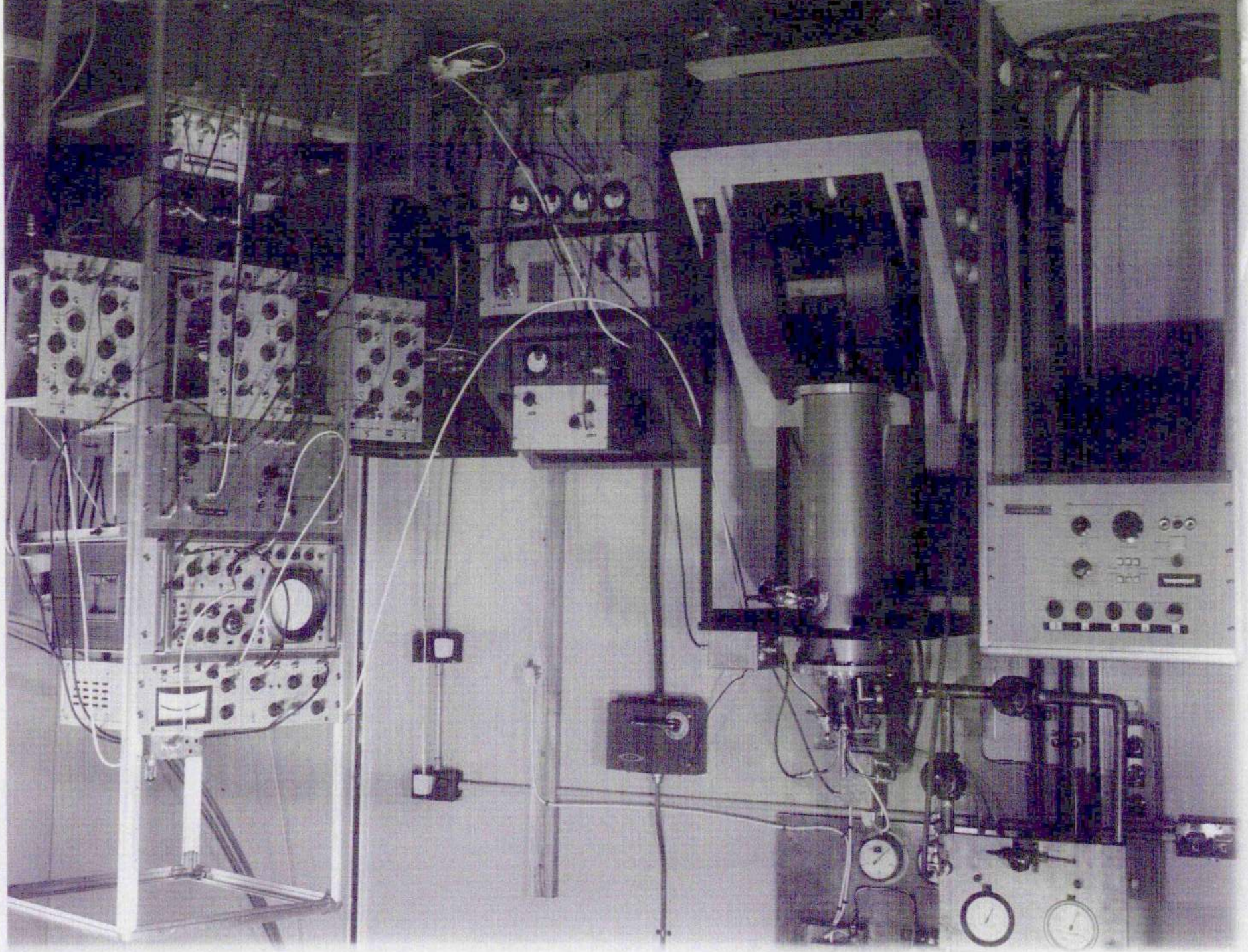

CONTENTS

CHAPTER I - INTRODUCTION

The discovery of nuclear magnetic resonance (n.m.r.) by Bloch, Hansen and Packard[1], and by Purcell, Torrey and Pound[2] in 1946 introduced to physics a powerful and very general tool for studying many varied properties of matter. In particular in solids n.m.r. can give information on such diverse properties as molecular motions, molecular structure, phase transitions, electronic structure, electron-nucleus interactions, spin diffusion, spin thermodynamics and many others.

This thesis is a record of an investigation of spin-lattice relaxation times in several pure metals as a function of temperature. Dipolar relaxation times as well as the more usual Zeeman relaxation times in Al, Cu, V, Cd, and Pt are reported. The general theory of spin-lattice relaxation in metals was formulated by Hebel and Slichter[3], and less precisely by Anderson and Redfield[4]. Both these groups produced measurements which conflicted with the predictions of the theory. This discrepancy has been investigated.

The results reported here are compared with present theoretical predictions. The analysis leads to a correction of previously published values of δ, the ratio of the Zeeman to the dipolar relaxation time. Information is also obtained on electron-electron effects and the limits of the applicability of the current theory of these effects, and on the relative importance of the different electron-nuclear interactions in some of the metals investigated.

CHAPTER II - NUCLEAR INTERACTIONS

2.1. Introduction

Magnetic nuclei in a non-ferromagnetic metal in a magnetic field can interact in many ways with their surroundings. A nucleus experiences a large effect due to the external magnetic field and a smaller effect due to the field produced by all its magnetic neighbours. If it possesses a quadrupole moment electric field gradients in the metal will affect it. These interactions are not peculiar to metals. What is peculiar to metals is the effect of the conduction electrons on the nuclei through their hyperfine coupling, or through dipolar coupling. It is these particular phenomena which make n.m.r. such a useful technique for studying the properties of conductors.

All the effects mentioned in the above paragraph will now be introduced in greater detail as they all play a very important part in the theory of the experiments described in this thesis.

2.2. Basic Interaction

A nucleus with magnetic moment $\underline{\mu}$ when placed in a magnetic field $\underline{H}$ is described quantum mechanically by a very simple Hamiltonian:

$$\mathcal{H} = -\underline{\mu}.\underline{H}$$

Defining the z-direction to be along the field H_o leads to

$$\mathcal{H} = -\gamma\hbar H_o I_z$$

where γ is the "gyromagnetic ratio," defined by the relationship

$$\underline{\mu} = \gamma\hbar\underline{I}$$

Since $\underline{\mu}$ and $\underline{I}$ are parallel γ is a scalar.

The eigenvalues of the above Hamiltonian are multiples of the eigenvalues of I_z. The allowed energies are thus:

$$E = -\gamma\hbar H_o m \quad (m = I, I-1, \ldots, -I)$$

These energies form a set of equally spaced levels, the separation between adjacent ones being $\gamma\hbar H_o$. It is well known [1,2] that these levels can be detected by applying an alternating magnetic field perpendicular to the static field H_o and observing the absorption of energy when the frequency is such that

$$\hbar\omega = \gamma\hbar H_o$$

or $$\omega = \gamma H_o$$

This absorption is known as nuclear magnetic resonance and the frequency defined by the above equation is known as the Larmor frequency.

Although the consideration of a single nucleus leads to a correct description of many systems, when dealing with solids all N spins must be considered. If each spin has total angular momentum $\hbar\underline{I}$ the Hamiltonian which describes the interaction with an external magnetic field $\underline{H}_o$ whose direction is along the z-axis is given by:

$$\mathcal{H}_z = -\gamma\hbar H_o \sum_{i=1} I_z^i$$

This is known as the Zeeman Hamiltonian.

2.3. Dipole-Dipole Interaction

From the above, the observation of the nuclear energy levels should lead to a perfectly sharp absorption line. That this is not the case is due mainly to the fact that each nucleus is not just in a static magnetic field H_o but also in a magnetic field produced by all the neighbouring nuclei. As this varies from nucleus to nucleus the absorption frequency also varies leading to a broad spectral line.

The classical interaction energy E between two magnetic moments $\underline{\mu}_1$ and $\underline{\mu}_2$ separated by a distance $\underline{r}$ is

$$E = \frac{\underline{\mu}_1 \cdot \underline{\mu}_2}{r^3} - \frac{3(\underline{\mu}_1 \cdot \underline{r})(\underline{\mu}_2 \cdot \underline{r})}{r^5}$$

Extending this to N spins leads to the dipolar Hamiltonian which has the form:

$$\mathcal{H} = \frac{1}{2}\sum_{j=1}^{N}\sum_{k=1}^{N}\left[\frac{\underline{\mu}_j \cdot \underline{\mu}_k}{r^3} - \frac{3(\underline{\mu}_j \cdot \underline{r}_{jk})(\underline{\mu}_k \cdot \underline{r}_{jk})}{r^5}\right]$$

This Hamiltonian can be expressed in a more useful form by transforming to spherical co-ordinates r, θ, ϕ and writing $\underline{\mu}_j$ and $\underline{\mu}_k$ in component form, using the raising and lowering operators I_+ and I_- to express I_x and I_y. This gives

$$\mathcal{H}_{dd} = \frac{1}{2}\sum_{j,k}\frac{\gamma_1\gamma_2\hbar^2}{r_{jk}^3}\left[A + B + C + D + E + F\right]$$

where
$$A = I_{jz}I_{kz}(1 - 3\cos^2\theta_{jk})$$

$$B = -\frac{1}{4}\left[I_j^+ I_k^- + I_j^- I_k^+\right](1 - 3\cos^2\theta_{jk})$$

$$C = -\frac{3}{2}\left[I_j^+ I_{kz} + I_{jz} I_k^+\right]\sin\theta_{jk}\cos\theta_{jk}e^{-i\phi_{jk}}$$

$$D = -\frac{3}{2}\left[I_j^- I_{kz} + I_{jz} I_k^-\right]\sin\theta_{jk}\cos\theta_{jk}e^{i\phi_{jk}}$$

$$E = -\frac{3}{4} I_j^+ I_k^+ \sin^2\theta_{jk}e^{-2i\phi_{jk}}$$

$$F = -\frac{3}{4} I_j^- I_k^- \sin^2\theta_{jk}e^{2i\phi_{jk}}$$

Although this form looks more cumbersome than before it is much more useful for the computation of matrix elements. The principal terms of the dipolar Hamiltonian are the A and B terms which commute with the Zeeman Hamiltoniam. Since commuting terms cannot exchange energy the two Hamiltonians would be completely decoupled but for the terms C, D, E and F which do not commute with I_z and lead to a small energy exchange between the two systems.

2.4. Quadrupole Interaction

A nucleus with spin greater than $\frac{1}{2}$ possesses a quadrupole moment which interacts with electric field gradients to produce a

perturbation of the nuclear energy levels. The quadrupole Hamiltonian has the form

$$\mathcal{H}_Q = \frac{e^2qQ}{4I(2I-1)}[3I_z^2 - I^2]$$

when the electric field gradient has axial symmetry along the z-axis. Q is the quadrupole moment of the nucleus and q is the field gradient defined by

$$eq = V_{zz} = \frac{\partial^2 V}{\partial z^2}$$

When the magnetic interaction is much larger than the quadrupole coupling it can be shown[5], using first order perturbation theory, that the centre of the resonance is not shifted but satellite lines appear due to energy levels other than $\frac{1}{2}, -\frac{1}{2}$ being shifted. When these satellites are not resolved they produce a broadening of the resonance[6].

In a metal having cubic symmetry there should be no electric field gradients at the nucleus and hence no quadrupole effects. However, defects or impurities in the crystal lattice will lead to field gradients so an imperfect cubic metal will have a broader resonance than a perfect crystal.

2.5. Electron Spin Interaction

The Hamiltonian describing the interaction of an electron with the nucleus can be written as

$$\mathcal{H}_{en} = \gamma_e \gamma_n \hbar^2 \underline{I} \cdot \left(\frac{\underline{l}}{r^3} - \frac{\underline{s}}{r^3} + \frac{3\underline{r}(\underline{s}.\underline{r})}{r^5} + \frac{8\pi}{3} \underline{s}\, \delta(\underline{r}) \right)$$

this includes the coupling between the nucleus and the orbital angular momentum of the electron, dipole-dipole coupling between the nucleus and an electron (zero for electrons with spherically symmetric wave functions), and the hyperfine contact coupling which is only non-zero for electrons with a finite probability of

being at the nucleus i.e. s - type electrons.

Some of the features peculiar to metals caused by this Hamiltonian will now be considered separately.

2.5.1. Knight Shift

It is found that the resonance frequency for nuclei in a metal is usually higher than the resonance frequency for the same nuclei in an insulator in the same magnetic field[7]. This frequency shift is called the Knight shift. It is caused mainly by s -type electrons. These electrons have a net polarization due to the external field and since they have a probability density at the nucleus, this polarization acts as an extra magnetic field at the nucleus. Thus the field required for resonance is lower than the field required for resonance in an insulator. The contact interaction is also responsible for the Knight shift due to core polarization[8]. The spin-up and spin-down core electrons are affected differently by the net polarization of the conduction electrons so the core electrons gain a net polarization themselves which appears at the nucleus as another extra field. In this case the shift can be either positive or negative depending on the character of the conduction electron wave functions.

Electrons with other than s -type character can also cause a Knight shift through their dipolar coupling to the nuclei[6], but only in non-cubic metals. This frequency shift depends on the angle between H_o and the crystalline axes so in a metal powder this anisotropy gives rise to an asymmetric broadened resonance line.

The coupling between the nuclei and the electron orbital angular

momentum also causes a frequency shift via the orbital magnetism[9]. This contribution is isotropic.

Detailed calculations of these Knight shifts can be found in many sources. Briefly the method is to start from the electron-nuclear coupling and compute, using first order perturbation theory, the energy due to this coupling using a wave function ψ which is a product of the many particle wave functions ψ_e and ψ_n of the electron and the nucleus. In the case of the contact interaction the energy computed is equivalent to the nucleus being in an extra magnetic field ΔH given in magnitude by

$$\frac{\Delta H}{H_o} = \frac{8\pi}{3} \left\langle \left| U_k(0) \right|^2 \right\rangle_{EF} \chi_e^s$$

and acting in such a way as to aid the external field H_o. $\left\langle \left| U_k(0) \right|^2 \right\rangle_{EF}$ is the density at the nucleus of s-type electrons on the Fermi surface and χ_e^s is the Pauli paramagnetic spin susceptibility.

2.5.2. Exchange Interaction

The spin density of the electron gas around a non-zero nuclear moment is not uniform. The presence of the magnetic moment at a lattice site makes that site more favourable for an electron of parallel moment. This is achieved by mixing in states of different wave number so that they interfere constructively at the nucleus. Going away from the nucleus these states get out of phase and produce beats or oscillations in the spin density. The range of such a rearrangement is such that the electron cloud round a neighbouring nucleus is affected and this in turn interacts with its

nucleus. When averaged over the conduction electron states the net effect is thus a nucleus-nucleus coupling via the electrons.[10,11]

The calculation of this effect is similar to the calculation of the Knight shift in that one starts with the electron-nuclear coupling and applies perturbation theory, in this case second order theory, to reduce t coupling to an effective interaction. Considering only s-state coupling on two nuclei $\underline{I}_1$ and I_2 we have:

$$\mathcal{H}_{en} = \frac{8\pi}{3}\left[\gamma_1\gamma_e\hbar^2\underline{I}_1\cdot\sum_1\underline{s}_1\,\delta(\underline{r}_1-\underline{R}_1) + \gamma_2\gamma_e\hbar^2\underline{I}_2\cdot\sum_1\underline{s}_e\,\delta(\underline{r}_e-\underline{R}_2)\right]$$

The use of a total wave function composed of electron and nuclear functions to compute the second order energy shift due to this Hamiltonian leads to an effective Hamiltonian of the form

$$\mathcal{H}_{eff} = -\frac{2}{9\pi}\gamma_e^2\gamma_1\gamma_2\hbar^2 m^*\left|U_{k_F}(0)\right|^4\frac{[\sin 2k_FR - 2k_FR\cos 2k_FR]}{R^4}\,\underline{I}_1\cdot\underline{I}_2$$

$$= A\,\underline{I}_1\cdot\underline{I}_2 = \mathcal{H}_{ex}$$

In arriving at this expression the assumption is made of spherical energy surfaces, an effective mass m* and the equality of $\left|U_{k'}(0)\right|^2\left|U_k(0)\right|^2$ to $\left|U_{k_F}(0)\right|^4$ since it is only when $k' = k = k_F$ that this produces a large contribution.

From the above it can be seen that the range of the interaction is relatively large. Also, because $\left|U_{k_F}(0)\right|$ is greater for atoms with large atomic numbers the coupling will become larger for the heavier elements. In fact in many cases it greatly exceeds the direct dipolar coupling.

In solids the main manifestation of this interaction is its effect on resonance linewidth or on a related measurement known

as the "second moment"[12]. When all the magnetic nuclei are identical the line is narrowed and the wings are enhanced leaving the second moment unchanged. If the nuclei are not identical the second moment is increased and the resonance curve is broadened. This gives rise to the terms "exchange narrowing" and "exchange broadening".

CHAPTER III - SPIN-LATTICE RELAXATION

3.1. Introduction

When nuclei are coupled to each other much more strongly than with the lattice it is well established[13] that the strong coupling establishes a common temperature for the spins. This common temperature is established in a characteristic time, T_2, know as the spin-spin relaxation time. If the temperature of the spins is different from the lattice temperature the weak lattice coupling will cause the spin temperature to change towards the lattice temperature with a time constant T_1, the spin-lattice relaxation time. Because the nuclear system is describable by a single parameter, T_s, it is reasonable to make the assumption that the recovery of the system towards equilibrium will be governed by a single time constant T_1 according to the relation

$$\frac{d\beta}{dt} = -\frac{1}{T_1}(\beta-\beta_o) \qquad (3.1)$$

where $\beta = \frac{1}{kT_s}$ and $\beta_o = \frac{1}{kT_L}$, T_s and T_L being the temperatures of the spins and the lattice respectively. This assumption can be shown to be implicit in the assumption of a spin temperature.

3.2. Derivation of Hebel-Slichter T_1 Formula

The relaxation time, T_1, or more strictly the relaxation rate, $\frac{1}{T_1}$, for a system describably by a spin temperature has been calculated for a general relaxation mechanism by Hebel and Slichter[3a,b] who generalised a similar calculation by Gorter.[14]

Consider a system of nuclear spins whose Hamiltonian, $\mathcal{H}$,

has eigenvalues E_n, and in which the fractional occupation of state n is p_n. (Thus n designates a state of the total system, rather than the energy of a single spin.) Since we require that the spins occupy at least one of the states n we must have

$$\sum_n p_n = 1 \qquad 3.2$$

The average energy of the system, $\bar{E}$, is then

$$\bar{E} = \sum_n p_n E_n \qquad 3.3$$

The relaxation rate is found by considering changes in the average energy, $\frac{d\bar{E}}{dt}$, by two different methods and equating the resultant expressions.

$$\frac{d\bar{E}}{dt} = \frac{d\bar{E}}{d\beta}\cdot\frac{d\beta}{dt} \qquad 3.4$$

and also

$$\frac{d\bar{E}}{dt} = \frac{d}{dt}\sum_n p_n E_n = \sum_n E_n \frac{dp_n}{dt} \qquad 3.5$$

Assuming that the p_n's obey simple linear rate equations and introducing W_{mn} as the probability per second that the lattice induces a transition of the system from m to n if the system is in state m, the rate equation is

$$\frac{dp_n}{dt} = \sum_m (p_m W_{mn} - p_n W_{nm}) \qquad 3.6$$

This leads to

$$\frac{d\bar{E}}{dt} = \sum_{m,n} (p_m W_{mn} - p_n W_{nm}) E_n$$

$$= \tfrac{1}{2}\sum_{m,n} (p_m W_{mn} - p_n W_{nm})(E_n - E_m) \qquad 3.7$$

Since the system is always describable by a temperature

$$\frac{p_n}{p_m} = e^{(E_m - E_n)\beta} \approx 1 - (E_n - E_m)\beta \qquad 3.8$$

When the spins are in equilibrium with the lattice, the transitions between every pair of levels are in equilibrium. The principle of detailed balance says that

$$p_m{}^L W_{mn} = p_n{}^L W_{nm} \qquad 3.9$$

or that

$$W_{mn} = W_{nm} \frac{p_n^L}{p_m^L} \doteq W_{nm}[1 - (E_n - E_m)\beta_L] \qquad 3.10$$

By substituting equations (3.8) and (3.10) into equation (3.7) we find that

$$\frac{d\bar{E}}{dt} \doteq \tfrac{1}{2}\sum_{m,n} p_m W_{mn}(E_n - E_m)^2(\beta - \beta_L) \qquad 3.11$$

Now

$$p_n = \frac{e^{-\beta E_n}}{\sum_n e^{-\beta E_n}}$$

$$\doteq \frac{1 - \beta E_n + \beta^2 E_n{}^2 \ldots\ldots}{\sum_n (1 - \beta E_n + \beta^2 E_n{}^2 \ldots.)}$$

$$\doteq \frac{1}{\sum_n \delta_{nn}} \qquad 3.12$$

To derive another expression for $\frac{d\bar{E}}{dt}$ requires that we evaluate $\frac{d\bar{E}}{d\beta}$

$$\frac{d\bar{E}}{d\beta} = \frac{d}{d\beta}\sum_n p_n E_n$$

$$\doteq -\frac{1}{\sum_n \delta_{nn}} \sum_n E_n{}^2 e^{-\beta E_n}$$

$$\doteq \frac{1}{\sum_n \delta_{nn}} \sum_n E_n{}^2 \qquad 3.13$$

Combining (3.4) with (3.13) gives the required expression for $\frac{d\bar{E}}{dt}$.

This is then equated to (3.11) with (3.12) substituted to give finally for the relaxation rate

$$\frac{1}{T_1} = \frac{\sum_{m,n} W_{mn}(E_m - E_n)^2}{\frac{1}{2}\sum_n E_n^2} \qquad 3.14$$

This is the Hebel-Slichter formula for $\frac{1}{T_1}$.

3.3. Relaxation of Nuclei in a Metal

In a metal the lattice, or infinite capacity thermal reservoir, with which the nuclear spin system is in contact, consists of the conduction electrons. It has been shown that the first order effect of the electron-nucleus coupling is to produce an extra magnetic field at the nucleus which shifts the resonance frequency. This extra field is the time average of the fluctuating fields caused by the motion of the electrons. This fluctuating field can cause nuclear transitions and so will cause the nuclei to relax towards equilibrium. If it is the same interaction which gives rise to the Knight shift and the relaxation mechanism it is not unreasonable to expect some simple relationship between the two effects.

For coupling to the conduction electrons we have a nuclear spin system initially in some state m going to a final state n and simultaneously there is an electron transition from a state of wave vector k, and spin orientation s, to a state k^1, s^1. Considering only s-state coupling the probability of this happening is obtained by treating this as a scattering problem.

The elementary probability is:

$$\omega_{mks,nk^1s^1} = \frac{2\pi}{\hbar} \left|(mks|V|nk^1s^1)\right|^2 \delta(E_i - E_f)$$

where

$$V = \frac{8\pi}{3}\gamma_e\gamma_n\hbar^2 \underline{I}.\underline{S}\,\delta(\underline{r})$$

Thus

$$\omega_{mn} = \frac{2\pi}{\hbar}\left(\frac{8\pi}{3}\gamma_e\gamma_n\hbar^2\right)^2 \sum_{p.q}(k|\delta(r_p)|k^1)(k^1|\delta(r_q)|k)$$

$$x\ \ [(m|I_p|n).(s|S|s^1)][(s^1|S|s).(n|I_q|m)]\delta(E_i - E_f)$$

where $\underline{I}_p$ and $\underline{I}_q$ are two nuclear spins separated from the electron by $\underline{r}_p$, $\underline{r}_q$. For the electron wave function a product of a spin function and a Bloch function is used, $U_k(\underline{r})e^{i\underline{k}.\underline{t}}$. The total probability per second of nuclear transitions is obtained by adding up the ω_{mn}'s for all initial and final electron states. This gives

$$W_{mn} = \sum_{\substack{ks\ \text{occupied} \\ k^1s^1\ \text{unoccupied}}} \omega_{nn}$$

The restrictions on ks and k^1s^1 can be removed by introducing the quantity p_{ks}, which is defined to be unity if ks is occupied; zero otherwise. This gives

$$W_{mn} = \sum_{\substack{k,s \\ k^1,s^1}} \omega_{mn}\, p_{ks}[1 - p_{k^1s^1}]$$

By averaging this equation over an ensemble of electron systems, p_{ks} is simply replaced by the Fermi function $f(E_{ks})$ to give

$$W_{mn} = \sum_{\substack{k,s \\ k^1,s^1}} \omega_{mn}\, f(E_{ks})[1 - f(E_{k^1s^1})]$$

The summation over k and k^1 can be replaced by an integral by defining a density of states function $\rho(E_k)$. The total probability is then found by integrating over d^3k and d^3k^1, and summing over the spin states $|s)$ and $|s^1)$. The assumption of high lattice temperature and a spherical Fermi surface leads finally to

$$W_{mn} = \sum_{p,q}{}' a_{pq} (m|I_p|n)(n|I_q|m)$$

with

$$a_{pq} = \frac{64}{9}\pi^3\hbar^3\gamma_e^2\gamma_n^2 \left\langle |U_k(0)|^2 \right\rangle_{E_F}^2 \frac{\sin^2 k_F R_{pq}}{(k_F R_{pq})^2} kT[\rho(E_F)]^2 \qquad 3.15$$

where k_F is the wave number at the Fermi surface and $\rho(E_F)$ is the density of states at the Fermi surface.

Substituting W_{mn} in the Hebel-Slichter formula (3.14) gives

$$\frac{1}{T_1} = -\tfrac{1}{2}\sum_{p,q}{}' a_{pq} \frac{\mathrm{Tr}([\mathcal{H}_0, I_p].[\mathcal{H}_0, I_q])}{\mathrm{Tr}\mathcal{H}_0^2} \qquad 3.16$$

where $\mathcal{H}_0$ is the total nuclear Hamiltonian and Tr stands for "the sum of the diagonal matrix elements."

3.3.1. Relaxation in High Field

The dominant term in the nuclear Hamiltonian in a large magnetic field is the Zeeman Hamiltonian. That it to say most of the energy of the nuclear spin system is in the form of Zeeman energy. A large field in this context means H_0 much greater than the field produced at one nucleus by its neighbours. Substituting $\mathcal{H}_z$ in (3.16) and neglecting a_{pq} for $p \neq q$ since these terms are much smaller than a_{oo} gives

$$\frac{1}{T_{1z}} = -\frac{a_{oo}}{2}\,\frac{\mathrm{Tr}[\mathcal{H}_z, I]^2}{\mathrm{Tr}\mathcal{H}_z^2}$$

$$= -\frac{a_{oo}}{2}\,\frac{-2\mathrm{Tr}\mathcal{H}_z^2}{\mathrm{Tr}\mathcal{H}_z^2}$$

$$= a_{oo}$$

Thus $$\frac{1}{T_{1z}} = \frac{64}{9}\pi^3\hbar^3\gamma_e^2\gamma_n^2\left\langle\left|U_k(0)\right|^2\right\rangle_{E_F}^2 \rho^2(E_F)kT \qquad 3.17$$

The quantity $\left\langle\left|U_k(0)\right|^2\right\rangle$ also appeared in the expression for the Knight shift

$$\frac{\Delta H}{H} = \frac{8\pi}{3}\left\langle\left|U_k(0)\right|^2\right\rangle\chi_e^s \qquad 3.18$$

These expressions have been arrived at by assuming a non-interacting electron gas. This same model gives for the electron spin susceptibility

$$\chi_{eo}^s = \frac{\gamma_e^2\hbar^2}{2}\rho_o(E_F) \qquad 3.19$$

where $\rho_o(E_F)$ is the total density of electron states in energy. Combining (3.17), (3.18) and (3.19) gives the expected simple relationship between the Knight shift and the relaxation time.

$$T_1T\left(\frac{\Delta H}{H}\right)^2 = \frac{\hbar}{4\pi k}\left(\frac{\gamma_e}{\gamma_n}\right)^2 = \text{constant}$$

This expression was first derived by J. Korringa[15] and is known as the Korringa relation. When many body effects in the electron gas were allowed for[16] this became

$$T_1T\left(\frac{\Delta H}{H}\right)^2 = \frac{\hbar}{4\pi k}\left(\frac{\gamma_e}{\gamma_n}\right)^2\left[\frac{\chi_e^s\rho_o(E_F)}{\chi_{eo}^s\rho(E_F)}\right]^2 \qquad 3.21$$

It will be shown in chapter 6 that this formula is not correct.

3.3.2. Relaxation in Low Field

When the external field is reduced to such a value that spin-spin interactions are comparable to the Zeeman interaction a more general nuclear Hamiltonian must be substituted in the relaxation equation (3.16). We will consider a Hamiltonian consisting of a Zeeman component $\mathcal{H}_z$ as in section (2.2), a spin-spin coupling Hamiltonian $\mathcal{H}_{ss} = \mathcal{H}_{dd} + \mathcal{H}_{ex}$ as in sections (2.3) and (2.5.2.), and a quadrupole component $\mathcal{H}_Q$ as in section (2.4). Neglecting a_{pq} where $p \neq q$ as before gives[17]:

$$\frac{1}{T_1} = a_{oo} \frac{\mathrm{Tr}\mathcal{H}_z^2 + 2\mathrm{Tr}\mathcal{H}_{ss}^2 + 3\mathrm{Tr}\mathcal{H}_Q^2}{\mathrm{Tr}\mathcal{H}_z^2 + \mathrm{Tr}\mathcal{H}_{ss}^2 + \mathrm{Tr}\mathcal{H}_Q^2} \qquad 3.22$$

This leads to some interesting conclusions.

In zero field where $\mathcal{H}_z = 0$, in the presence of only a dipolar Hamiltonian

$$\frac{T_{1z}}{T_{1dd}} = \delta = 2$$

If we have only a quadrupolar Hamiltonian then

$$\frac{T_{1z}}{T_{1Q}} = 3$$

When both interactions are present the ratio should lie between 2 and 3, the actual value depending on the relative strengths of the couplings.

These conclusions are based on the assumption of the incoherence of local field, that is the field due to an electron at one nucleus is uncorrelated to the field at another nucleus. This assumption is implicit in the neglect of a_{pq} when $p \neq q$. When these terms are included the conclusions are altered very little, the only difference

being that

$$\frac{T_{1z}}{T_{1dd}} = \delta \sim 2.01 \text{ for most metals}$$

By including the a_{pq} terms we have allowed for the fact that the electrons are not localised but have wavelengths which are comparable to the interatomic distance. Thus we are allowing for overlap but are still making the assumption that thhe electrons are non-interacting.

A theoretical treatment of δ, allowing for electron-electron interactions, has been given by Wolff[18]. Using a delta function to represent the interaction he related the electron spin correlation function to the non-local electron spin susceptibility. His expressions may be summarised:

$\delta = 2 + \epsilon$ (in the case of dipolar relaxation alone)

$\delta = 2 - 2\epsilon$ (in the case of exchange relaxation alone)

where

$$\epsilon = [\sum_{jk} (K_{jk}/r_{jk}^{6}) / \sum_{jk} (1/r_{jk}^{6})]$$

r_{jk} being the distance between two nuclei, j and k, and K_{jk} being given by

$$K_{jk} = \frac{\frac{1}{x_{jk}} \int_0^1 \sin(qx_{jk})(1 - \alpha f(q))^{-2} dq}{\int_0^1 q(1 - \alpha f(q))^{-2} dq} \qquad 3.23$$

where $q = Q/2k_F$, Q being the amplitude of the wave vector in the susceptibility function; $x_{jk} = 2k_F r_{jk}$, k_F being the wave number at the Fermi surface; α is an enhancement parameter proportional to the strength of the electron-electron interactions; and

$f(q) = \frac{1}{2}[1 + \frac{(1+q^2)}{2q} \ln (\frac{1+q}{1-q})]$ is the q-dependent factor in the real part of the susceptibility of a non-interacting electron gas. This expression is valid only for metals whose Fermi surface is almost spherical and is contained in the first Brillouin zone. Before applying this formula a value of α must be found by comparing the calculated free electron susceptibility with the measured or theoretical value[16] of the actual susceptibility.

The difference in δ between the two forms of the spin-spin coupling, dipolar and exchange, can be seen by evaluating equation (3.16) in full. The only non-zero traces when a Hamiltonian bi-linear in spins is used are:

$$\frac{1}{T_1} = \tfrac{1}{2}a_{11}\frac{\mathrm{Tr}[\mathcal{H},I_1]^2}{\mathrm{Tr}\mathcal{H}^2} - \tfrac{1}{2}a_{22}\frac{\mathrm{Tr}[\mathcal{H},I_2]^2}{\mathrm{Tr}\mathcal{H}^2} - \tfrac{1}{2}a_{12}\frac{\mathrm{Tr}[\mathcal{H},I_1][\mathcal{H},I_2]}{\mathrm{Tr}\mathcal{H}^2}$$

$$- \tfrac{1}{2}a_{21}\frac{\mathrm{Tr}[\mathcal{H},I_2][\mathcal{H},I_1]}{\mathrm{Tr}\mathcal{H}^2} = -a_{11}\frac{\mathrm{Tr}[\mathcal{H},I_1]^2}{\mathrm{Tr}\mathcal{H}^2} - a_{12}\frac{\mathrm{Tr}[\mathcal{H},I_1][\mathcal{H},I_2]}{\mathrm{Tr}\mathcal{H}^2}$$

When $\mathcal{H} = \mathcal{H}_{dd}$

$$\frac{\mathrm{Tr}[\mathcal{H}_{dd},I_1]^2}{\mathrm{Tr}\mathcal{H}_{dd}^2} = -2\,, \qquad \frac{\mathrm{Tr}[\mathcal{H}_{dd},I_1][\mathcal{H}_{dd},I_2]}{\mathrm{Tr}\mathcal{H}_{dd}^2} = -1$$

When $\mathcal{H} = \mathcal{H}_{ex} = A\underline{I}_1 \cdot \underline{I}_2$

$$\frac{\mathrm{Tr}[\mathcal{H}_{ex},I_1]^2}{\mathrm{Tr}\mathcal{H}_{ex}^2} = -2\,, \qquad \frac{\mathrm{Tr}[\mathcal{H}_{ex},I_1][\mathcal{H}_{ex},I_2]}{\mathrm{Tr}\mathcal{H}_{ex}^2} = 2$$

Noting that $\frac{1}{T_{1z}} = a_{11}$

Then[19]

$$\frac{T_{1z}}{T_{1dd}} = 2 + \frac{a_{12}}{a_{11}} = 2 + \epsilon$$

$$\frac{T_{1z}}{T_{1ex}} = 2 - 2\frac{a_{12}}{a_{11}} = 2 - 2\epsilon$$

In the unlikely occurence of complete correlation between local fields a_{12} would equal a_{11} and we would have $\delta = 3$ for dipolar relaxation and $\delta = 0$ for exchange relaxation. The fact that the exchange relaxation time becomes very long in the presence of correlations can be seen from the form of the exchange coupling, $\underline{I}_1 \cdot \underline{I}_2$. If the electron field at nucleus 1 is the same as at nucleus 2 the nuclei will be flipped simultaneously. This means the angle between them does not change so their energy is constant.

3.3.3. Other Relaxation Mechanisms

Although the contact hyperfine interaction is the most important relaxation mechanism in most metals there are exceptions where other mechanisms can dominate. Just as other interactions can cause a frequency shift these same interactions can cause relaxation. Thus it is possible to have relaxation via a core-polarization interaction, via a dipolar interaction to non s-type electrons, or via an orbital interaction. All these relaxation times are related to the corresponding frequency shifts by Korringa-like relations except the orbital interaction.

When there is no correlation between neighbouring local fields the value of δ is independent of the relaxation mechanism, that value being $\delta \doteqdot 2$.. In the presence of correlations present theories deal only with relaxation by the contact hyperfine interaction. It is possible that the value of δ would be modified if other relaxation processes were considered.

3.4. Methods of Measuring T_{1dd}

All references to T_{1dd} in the previous section (3.3) have implied that this is the value of T_1 measured in zero field. This is true, but a more general description of T_{1dd} would be the relaxation time for the return of the dipolar energy reservoir to equilibrium. In high field most of the spin energy is in the Zeeman system since this represents an interaction of about 1 tesla as opposed to the dipolar interaction of about 10^{-4} tesla. Thus usually it is not possible to see a signal from the dipolar energy bath. All measurements of T_{1dd} require firstly a method of transferring energy from the large Zeeman reservoir to the dipolar reservoir, and secondly a method of detecting this energy in order to follow the variation with time.

The first measurements of T_{1dd}[3,4] were performed using a field cycling technique. This involved polarizing the spins for a long time in high field to ensure a large Zeeman energy bath then adiabatically demagnetising into zero field to transfer order into the dipolar system. After a known time the sample was remagnetised, again adiabatically, to transfer the remaining dipolar energy back into Zeeman energy. The signal obtained on remagnetising depended on the amount of relaxation in zero field so giving a measure of T_{1dd}. Because of the times required to switch large magnetic fields only times longer than about one hundred milleseconds could be measured in this way.

All subsequent measurements were made in high field. A common

technique is one very similar to the method above except that the spins are adiabatically demagnetised to zero field in the rotating frame[20,21,22] by switching off an r.f. field. The amount of order in the dipolar system is observed by adiabatically switching the r.f. field back on then switching off suddenly. The height of the resulting induction decay is a measure of the energy of the dipolar spins.

Another method, introduced by Jeener and Brockaert[23] involves a double pulse sequence to transfer order irreversibly from the Zeeman system to the dipolar system.

Consider a spin system whose Hamiltonian consists of a Zeeman part, $\mathcal{H}_z$, and a dipolar part, $\mathcal{H}_{dd}$, which can be divided into a part, $\mathcal{H}'_{dd}$, which commutes with $\mathcal{H}_z$ and a part, $\mathcal{H}''_{dd}$, which does not commute with $\mathcal{H}_z$. The total Hamiltonian is then

$$\mathcal{H} = \mathcal{H}_z + \mathcal{H}'_{dd} + \mathcal{H}''_{dd}$$

By assuming the existance of a dipolar temperature T_D and a Zeeman temperature T_z the system can be described by a density matrix whose high-temperature approximation is

$$\rho = \beta\left(1 - \mathcal{H}'/kT_D - \mathcal{H}_z/kT_z\right)$$

where β is a normalisation constant.

The energy of the system can now be written as the sum of the Zeeman energy and the dipolar energy

$$E = E_D + E_z$$

where

$$E_D = \mathrm{Tr}(\mathcal{H}'_{dd}\,\rho) = -(1/kT_D)\,\beta\,\mathrm{Tr}(\mathcal{H}'^{2}_{dd}) = -(1/kT_D)\mathcal{D}^2$$

$$E_z = \mathrm{Tr}(\mathcal{H}_z\,\rho) = -(1/kT_z)\,\beta\,\mathrm{Tr}(\mathcal{H}^2_z) = -(1/kT_z)Z^2$$

If a short intense Θ pulse of transverse r.f. magnetic field is applied to this system at the Larmor frequency, the resultant transient transverse magnetisation has the form[24] (in a reference frame rotating round H_o at the Larmor frequency)

$$M_x(t) = \gamma\hbar(E_z/Z)(\sin\Theta)\, g(t) \qquad 3.24.1$$

$$M_y(t) = \gamma\hbar(E_D/\mathcal{D})\, F(t,\Theta) \qquad 3.24.2$$

where

$$g(t) = \mathrm{Tr}\left(I_x Q(t)(\gamma\hbar H_o)\, I_x Q^{-1}(t)\right) / \left|(\rho\, \mathrm{tr}(\mathcal{H}_z)^2)^{\frac{1}{2}}\right|$$

$$F(t,\Theta) = \mathrm{Tr}\left(I_y Q(t) R(\Theta,\pi/2)\mathcal{H}'_{dd} R^{-1}(\Theta,\pi/2) Q^{-1}(t)\right) / \left|(\rho\, \mathrm{Tr}(\mathcal{H}'_{dd})^2)^{\frac{1}{2}}\right|$$

$$R(\Theta,\Phi) = \exp\left[-i\Theta(I_x\cos\Phi + I_y\sin\Phi)\right]$$

$$Q(t) = \exp\left[-(it/\hbar)\mathcal{H}_{dd}\right]$$

It is obvious from equation (3.24.1) and equation (3.24.2) that the Zeeman and dipolar components of the voltage induced in a pick-up coil in the x-axis of the laboratory frame will have orthogonal phases. Thus the use of a phase-sensitive receiver will lead to the separation and independent observation of either component. Normally in a high field the dipolar energy is so small that the signal is zero from a receiver sensitive only to r.f. out of phase with the Zeeman component.

Jeener and Brockaert have shown[23] that the application of a pair of orthogonal pulses of certain widths leads to a non-zero efficiency of transfer of Zeeman order to dipolar order. The return to equilibrium of the dipole energy bath can then be observed by applying a third pulse and looking at the signal with the receiver

set for the proper phase. With this technique order can be transferred in a time of a few T_2's which is only several hundred microseconds so relaxation times of milleseconds can be measured. This represents a large advantage over other methods and is the main reason that this technique was adopted for the work described in this thesis. A disadvantage is the loss of signal over other methods as the maximum efficiency is about 50%.

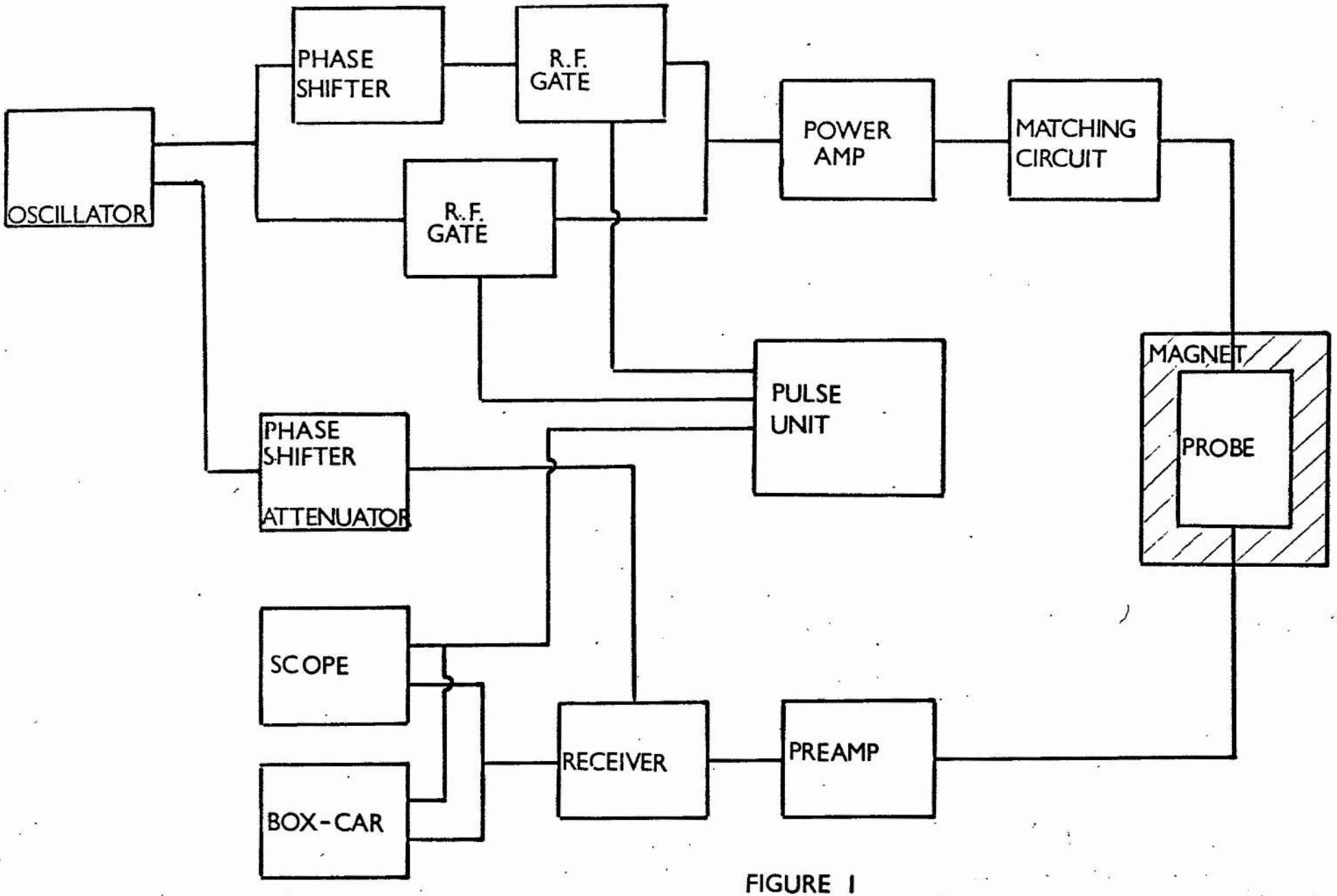
PHASE SHIFTER
R.F. GATE
OSCILLATOR
R.F. GATE
POWER AMP
MATCHING CIRCUIT
MAGNET
PROBE
PULSE UNIT
PHASE SHIFTER
ATTENUATOR
SCOPE
BOX-CAR
RECEIVER
PREAMP

FIGURE 1

CHAPTER IV - APPARATUS

4.1. Introduction

The Jeener technique requires an apparatus capable of producing variable length, variable phase, radio frequency pulses, and a receiver which is sensitive to the phase as well as the amplitude of the resulting signal. Measurement of the dipolar relaxation time requires the observation of a small decaying signal which is out of phase with a larger growing Zeeman signal.

Any drift in phase or field could lead to large errors. For this reason good stability is required from both the radio frequency generator and the static magnetic field.

These specifications were all satisfied by our apparatus which is shown in block diagram form in figure 1. The components of the spectrometer will be described individually.

4.2. Oscillator and Gate

Based on a design by Blume[25], the oscillator (figure 2) was crystal controlled and had a frequency stability greater than 1 in 10^6 after an initial warm-up period. The master frequency was 10.0022 MHz. The oscillator was carefully screened in a box of 1/8 in thick copper and all co-axial leads from the box were double screened to ensure that leakage was kept to a minimum. The output from the cathode of V1b was lead not only to the anode of V2 but also through double screened cable to a delay line housed in another copper box and hence to the anode of the gating valve in the second gate. The delay line was an AD-YU Electronics type

FIGURE 2

Unless noted, all resistors are $\frac{1}{2}$W

All capacitors

< 1 are in μF

>1 are in pF

Power from Textronix 160A

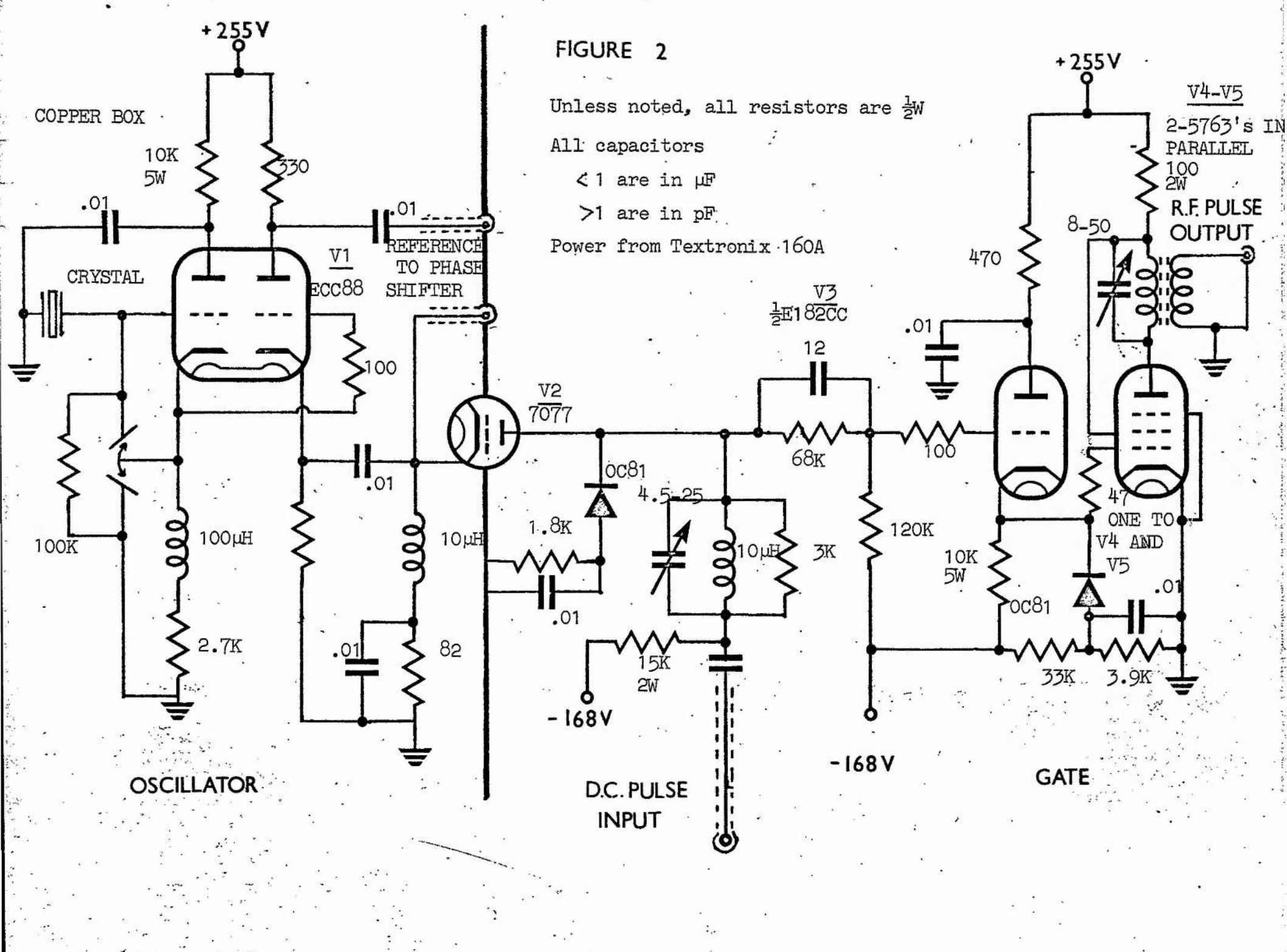

557k with a total delay of 0.1μs and thus 360° variation in phase.

The input to the gate was a.c. coupled to the pulse amplifiers but long pulses could be obtained by d.c. coupling the input to a modified pulse amplifier. The output was transformer coupled and adjusted to present an impedance of about 100 ohms so that the two gates in parallel presented 50 ohms to the next stage ensuring optimum power transfer.

4.3. Power Amplifier

The total power amplifier consisted of three separate units. The outputs from the r.f. gates were fed into a 5 watt amplifier which drove a 90 watt amplifier. This in turn drove the final stage which was capable of producing one kilowatt of power into a 50 ohm load.

All the amplifiers used the same basic design (figure 3a) which was based on circuits described in the Radio Amateurs Handbook.[40] The pulse passes through a tuned grid to the valve, or valves in the final stage, where it is amplified and then matched to the next stage through a pi network. Care was taken to ensure that all the tuned circuits had a sufficiently wide bandwidth to facilitate the passage of a square pulse. For this reason i.e. square pulses, and also for maximum efficiency and maximum suppression outwith the pulses, all the amplifiers were operated in class C.

The final stage had an output impedance of 50 ohms which had to be matched to the high impedance of the tuned circuit containing the transmitter coil. An L matching circuit, shown in figure 3b,

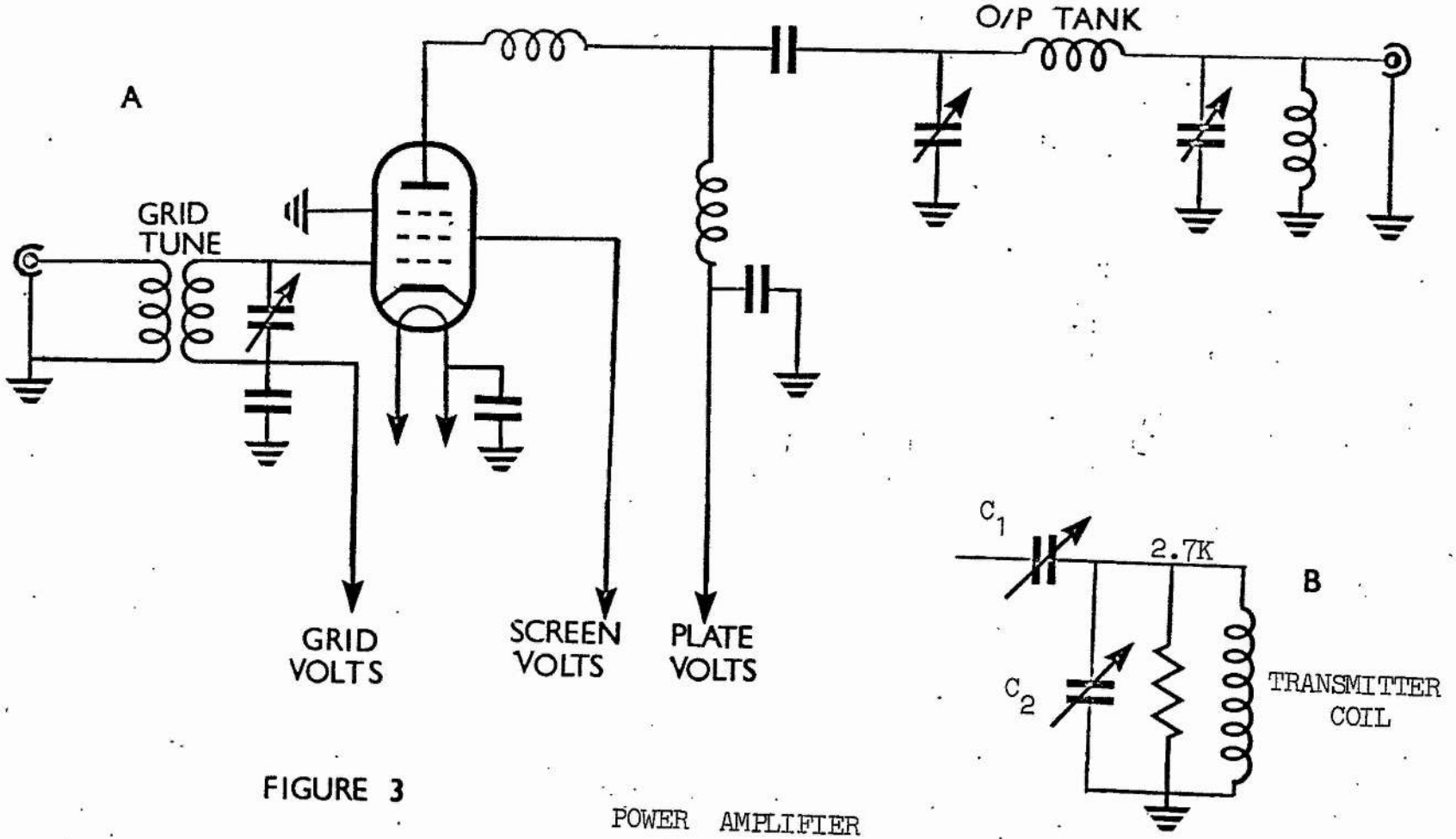

FIGURE 3

POWER AMPLIFIER

DESIGN.

was used. The resistor R was used to damp the coil and thus prevent excess "ringing" after the pulse. This was necessary to prevent the receiving system from being overloaded for a long time after the pulse. Both C_1 and C_2 were used to tune the coil.

With the transmitter fully tuned and no damping resistor across the coil a pulse of about five kilovolts could be obtained. In this condition a 90° pulse in aluminium lasted for 4μs corresponding to a rotating r.f. field of .006 tesla. Unfortunately the dead time of the receiver was about 40μs measured from the end of the pulse. With a damping resistor of 2.7 kilohms a 90° pulse of 10μs was obtained with only 20 μs dead time after the pulse. This was adequate for most metals. The rise and fall times of the pulse were both about 2μs.

4.4. Pre-Amplifier

Each stage of an amplifier chain has an individual noise factor and power gain. If these are given by F_1, F_2, ..., F_n and P_1, P_2, ..., P_n respectively then the overall noise factor, F_o is given by

$$F_o = F_1 + \frac{F_2-1}{P_1} + \frac{F_3-1}{P_1 \cdot P_2} + \ldots\ldots \frac{(F_n-1)}{(P_n-1)}$$

Usually P_1, P_2, ... are greater than unity so for most practical cases this expression can be truncated after the second term. Thus for the lowest overall noise factor, the noise factor of the first stage should be as low as possible and the power gain of the first stage should be as large as possible.

These conditions are met in n.m.r. by using a suitable

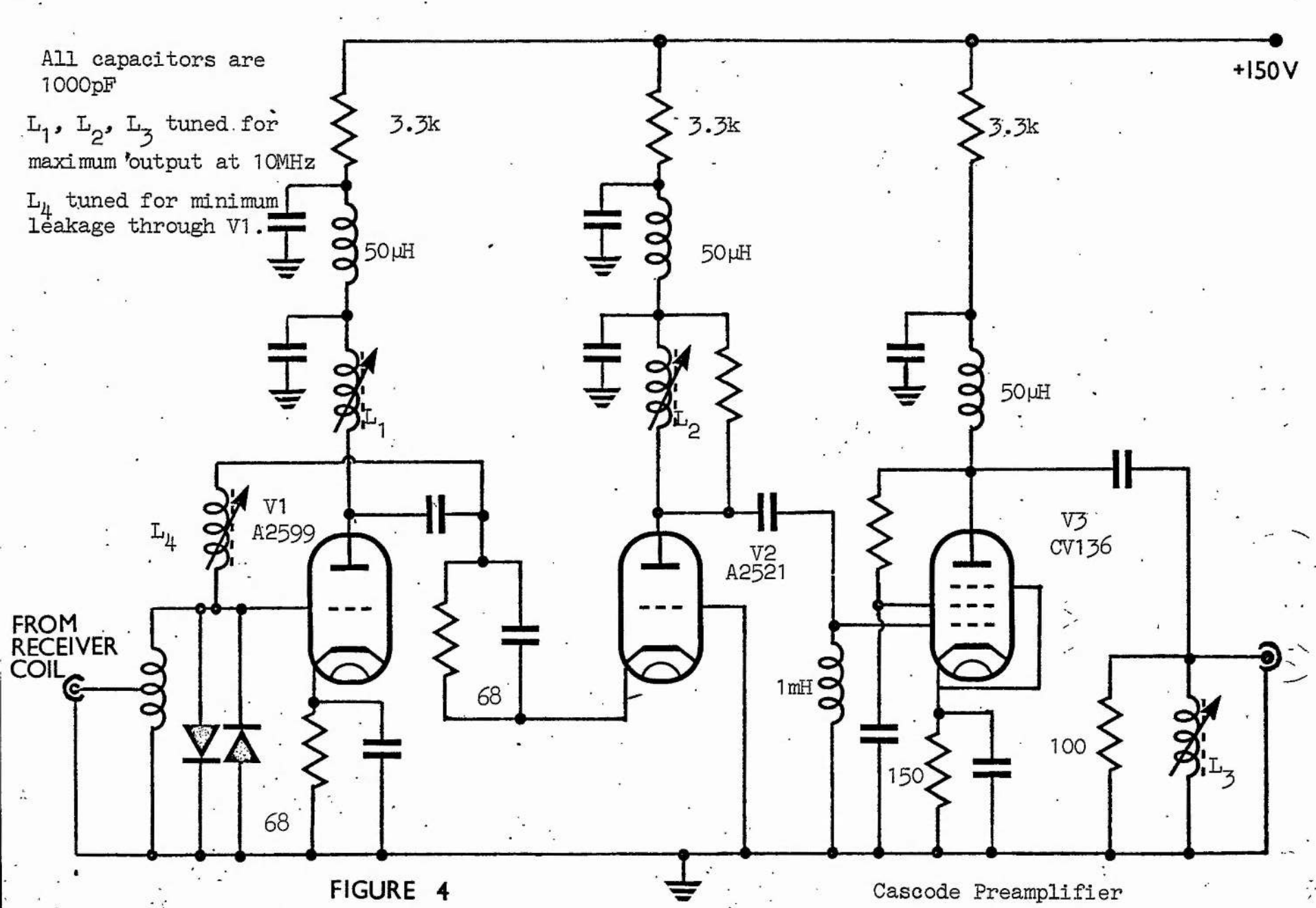

FIGURE 4

Cascode Preamplifier

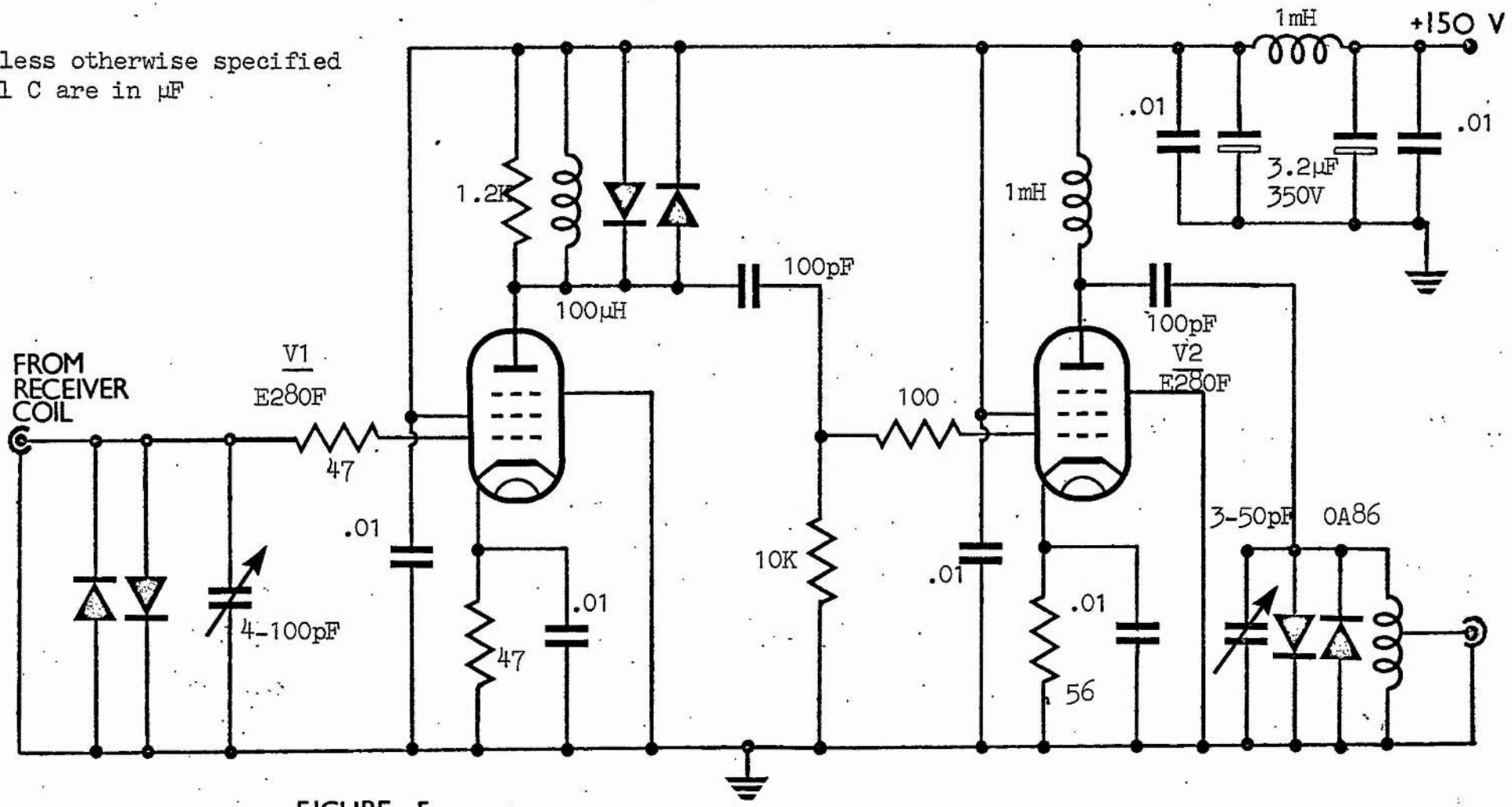
Unless otherwise specified
all C are in µF
FROM
RECEIVER
COIL
V1
E280F
47
.01
4-100pF
1.2K
100µH
47
.01
100pF
10K
100
1mH
.01
3.2µF
350V
1mH
+150 V
.01
100pF
V2
E280F
.01
56
3-50pF
0A86

FIGURE 5

preamplifier before the main receiver. However another condition must also be met. The coupling between the receiver and transmitter coils, although adjusted for a minimum, was of the order of 100:1 so that during a pulse 30 volts or more appeared at the input to the preamplifier, normally expected to amplify microvolts. Thus as well as having high gain and low noise the preamplifier must also recover quickly from a large overload so that the nuclear signal just after the pulse can be seen.

Two preamplifiers were used in the course of this work. The first was a cascode double triode amplifier shown in circuit form in figure 4. The overall noise figure obtained using this was such that the thermal noise generated in the receiver coil contributed more than the amplifier itself except at low temperatures. The input was protected from an overload by using crossed solid state diodes which prevent voltages greater than 0.5 volts from appearing there due to their low impedance. Due to the excessive anode current drawn by the last valve during a pulse these had very limited life-times. The inconvenience of the slow degradation in signal led to this preamplifier being abandoned except for some c.w. measurements for which it was well suited.

The second preamplifier was designed to have a high gain, low noise first stage and this was acheived by using a E280F pentode which has a very low equivalent series shot noise resistance. The circuit is shown in figure 4. The noise figures of the two preamplifiers were never measured quantitatively but a comparison of the signals obtained from each showed that the second one had the

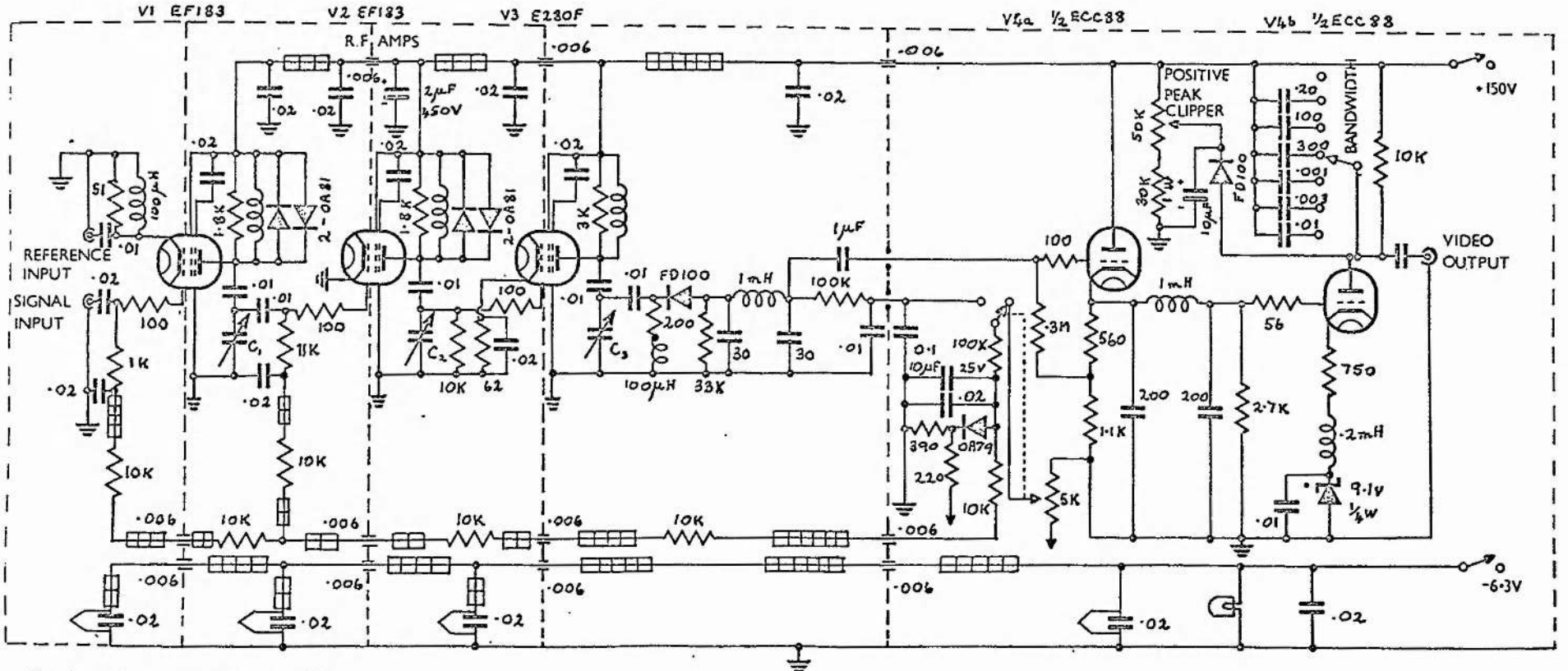

$C_1 = C_2 = C_3 \approx 5\text{-}20\,pF$ TRIMMER

$C > 1$ IN pF $\quad C \leq 1$ IN μF

FIGURE 6A RECEIVER

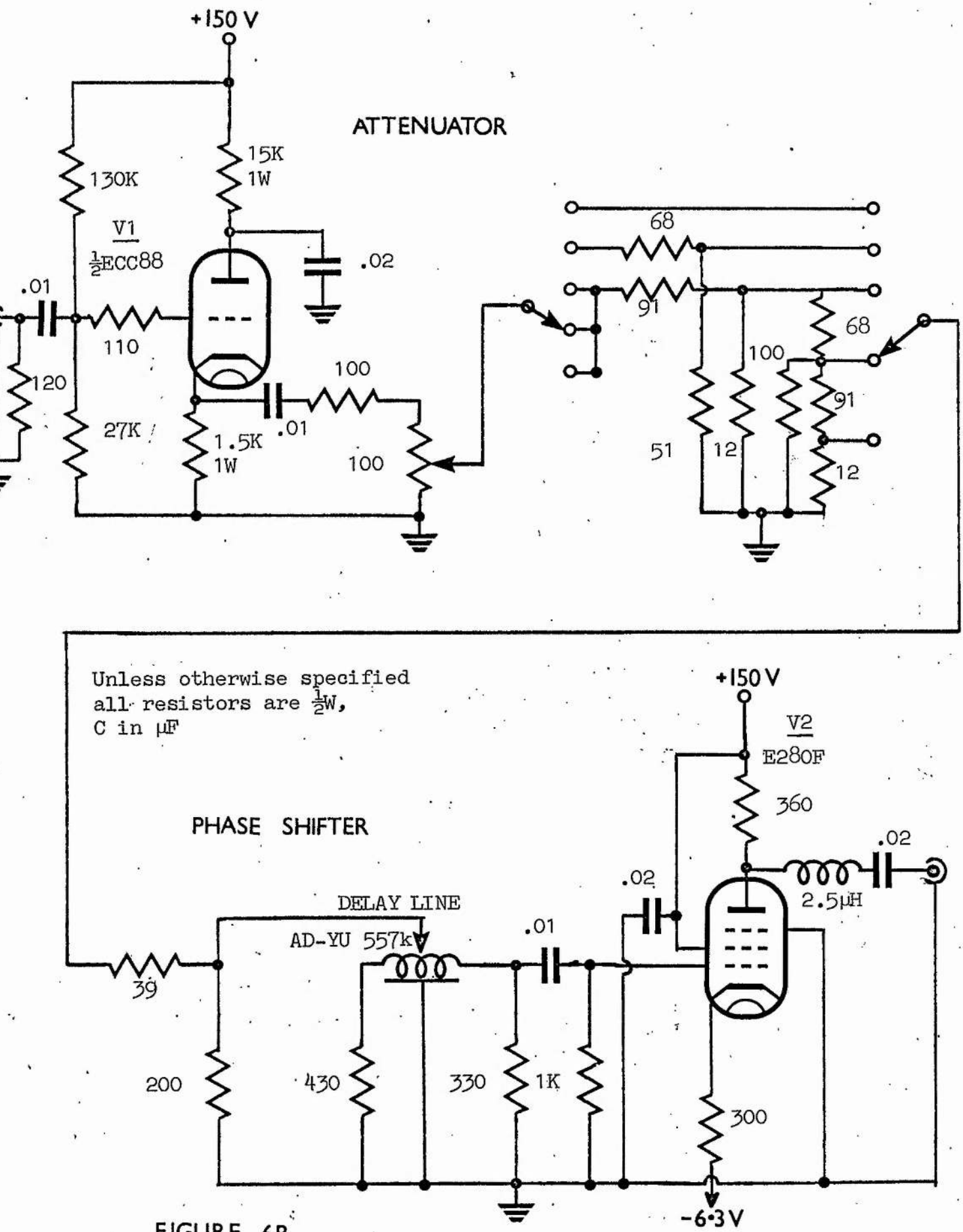
+150 V
ATTENUATOR
130K
15K
1W
V1
½ECC88
.01
.02
110
120
27K
1.5K
1W
.01
100
100
68
91
68
100
91
51
12
12
Unless otherwise specified
all resistors are ½W,
C in μF
+150 V
V2
E280F
PHASE SHIFTER
360
.02
.02
2.5μH
DELAY LINE
AD-YU 557k
.01
39
200
430
330
1K
300
-6·3 V

FIGURE 6B

better noise figure. Crossed diodes were used throughout to protect each stage. The output was transformer coupled into a long length of coaxial cable and so into the low input impedence receiver. Damping the receiver coil produced no effect on the recovery time but reduced the overall gain so this was left undamped. The overall small signal gain was about 100.

4.5. Receiver

The receiver (figure 6a) is a duplicate of the receiver described by Clark[26] except that it operates at a fixed frequency of 10 MHz. This receiver includes automatic gain control to provide a stable output. Overload is prevented by using crossed diodes as before. The nature of the receiver is such that linear operation is obtained if the signal does not escees 35% of the reference. The maximum gain of the three r.f. stages is about 2×10^3 and the gain of the video stage is about 8. Recovery from overload at maximum bandwidth takes place in less than 1μs, measured by comparing the output with the envelope of the input. The r.f. output stage was responsible for a varying d.c. level on the output so this stage was removed from the circuit.

4.5.1. Phase Shifter-Attenuator

This component (figure 6b) , a necessary part of the receiver, is also a copy of the model described by Clark in his paper. The output from the attenuator channel is fed into the phase shift channel. There is only one output which goes to the reference input of the receiver. At 10 MHz the output has a full 360° variation of phase, the VSWR being less than 1.3.

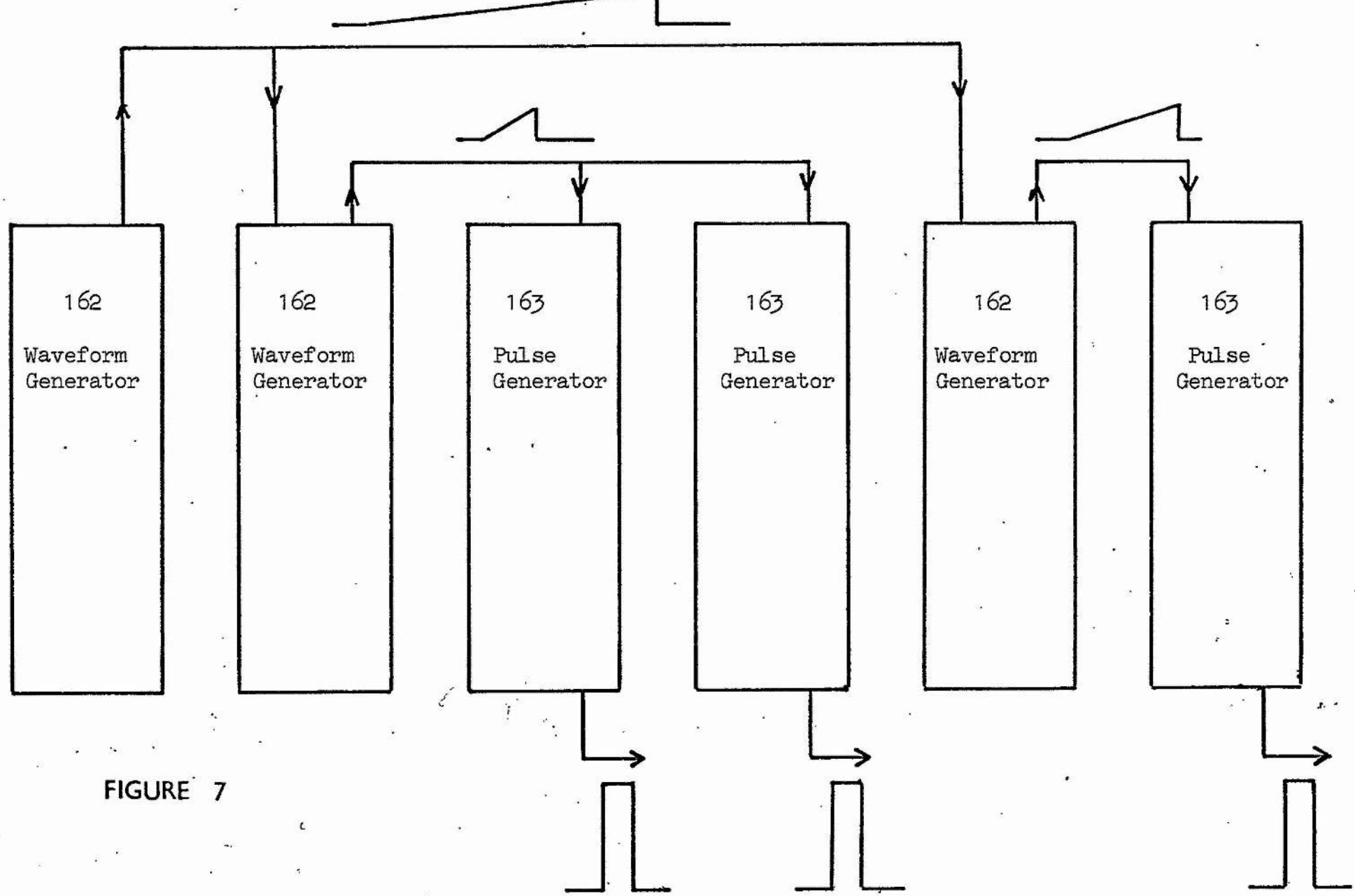
162
Waveform Generator
162
Waveform Generator
163
Pulse Generator
163
Pulse Generator
162
Waveform Generator
163
Pulse Generator

FIGURE 7

4.6. Measuring Devices

The output from the receiver was observed on a Hewlett-Packard 141A oscilloscope with variable persistance screen. The signal was also sampled by a P.A.R. Box-car Integrator, a device for measuring the height of a preselected part of the signal whilst greatly improving the signal to noise ratio. Had a phase coherent receiver not been required specifically to separate the two components of the signal, the utilisation of the full potential of the Box-car requires the use of such a receiver[27]. Since the Box-car is a relatively insensitive instrument, for the smaller signals a further audio amplifier was required after the receiver. This was a simple amplifier using an ECC88 and producing a gain of 14.

4.7. Pulse Units

The pulse units consist of a bank of Tektronix pulse and waveform generators arranged in such a way as to produce a stable three pulse sequence. From figure 7 it can be seen that the 162 waveform generator on the left controls the overall repetition rate. This triggers the other 162's simultaneously. The second left generator produces a short ramp which is fed into two of the 163 pulse generators. These each produce a pulse at a settable position on this ramp so the separation can be adjusted smoothly and accurately over any desired range. The second right unit produces a ramp which covers the time scale of the measurements. This is fed into the right 163 which can produce a pulse anywhere on this ramp.

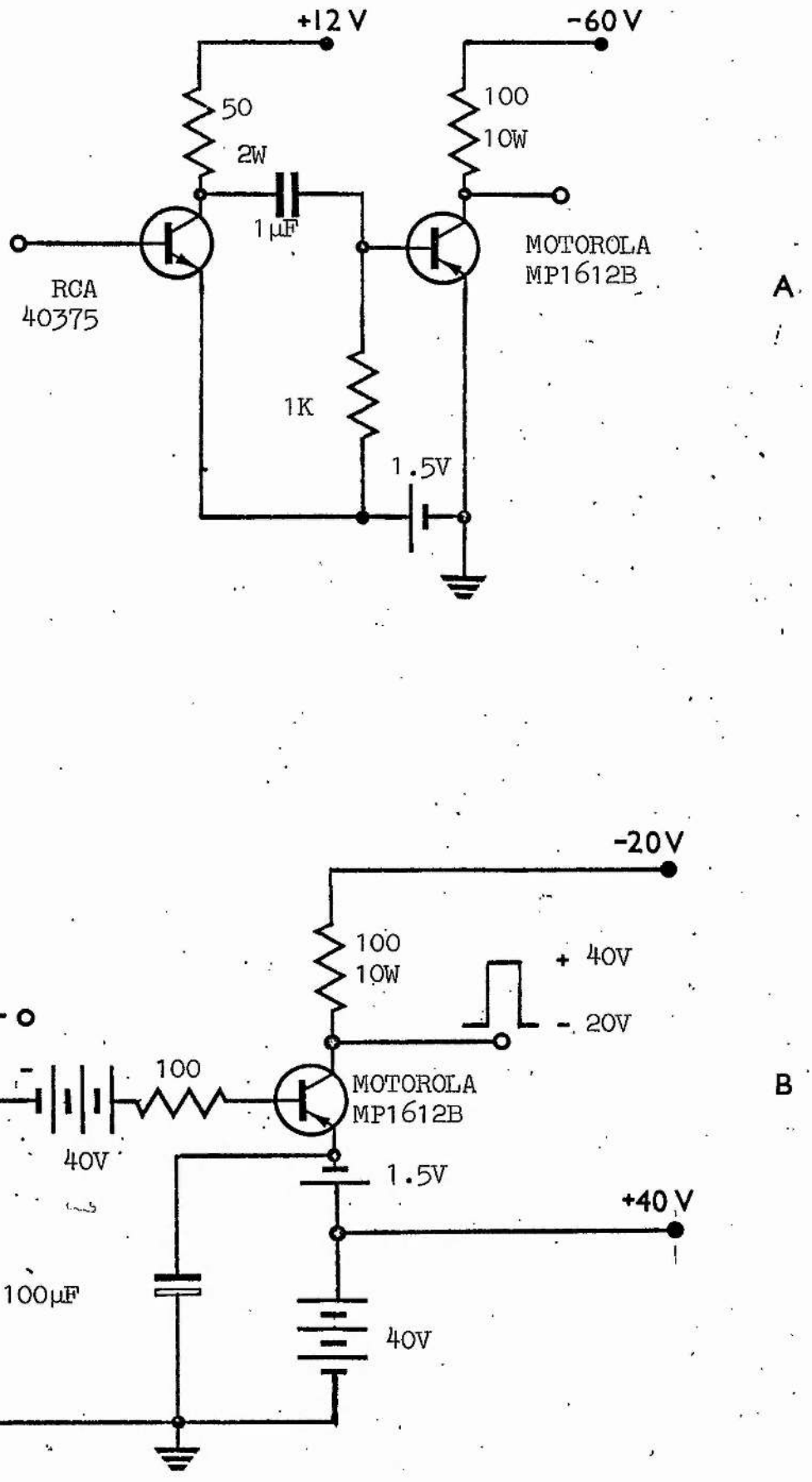
+12 V
-60 V
50
2W
100
10W
1 µF
RCA
40375
MOTOROLA
MP1612B
A
1K
1.5V
-20V
100
10W
+ 40V
- 20V
100
MOTOROLA
MP1612B
B
40V
1.5V
+40 V
100µF
40V

FIGURE 8

Thus we have a unit capable of producing two closely spaced pulses followed by a third pulse at a variable time later. This is just what is required to measure dipolar relaxation times using Jeener's technique. A two pulse sequence is generated by removing one of the centre 163 generators.

The pulses produced by these units, although of the correct polarity, are not powerful enough to trigger the r.f. gates so they must first be amplified by a two stage pulse amplifier. This amplifier could be modified to produce long pulses which were fed directly into the r.f. gate. The amplifier and the modification are shown in fugure 8a and figure 8b respectively.

4.8. Probe

Two probes were used in the course of the experiment but both were very similar. Lack of space in a second cryostat made the second probe necessary. Because of the similarity of the two probes only one will be described in detail. A crossed coil arrangement was chosen because with this system the different requirements of the transmitter and receiver coil are more easily met. Also the decoupling, being geometric is less liable to drift than the alternative methods such as a bridge or a phase shifter-attenuator.

The transmitter coil consisted of twelve turns, wound six on each cylindrical former, of 26 gauge copper wire. The receiver coil consisted of twelve turns of 38 gauge silver wire wound round the sample chamber separated from the sample by a perspex walls

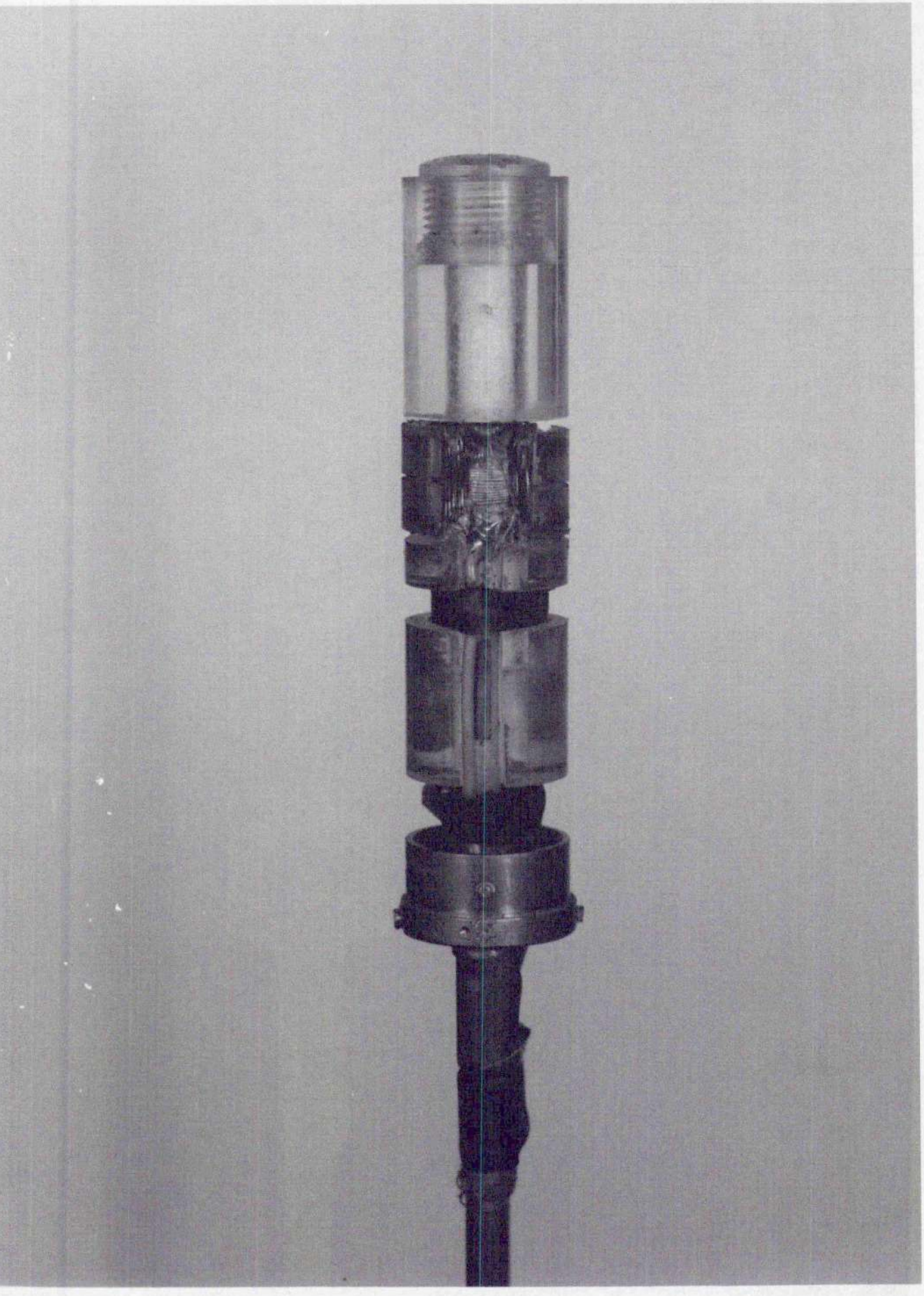

only a few thou thick. Silver wire was chosen because its resonance frequency is well separated from the frequencies of the samples studied.

4.9. Cryostat

Two cryostats were used. Both were metal liquid helium dewars with extension tails obtained from the Oxford Instrument Company. The main difference between the two was the diameters of their extension tails. Temperatures in the liquid air and room temperature regions were measured on a thermo-couple placed as near the sample as possible.

Using only liquid nitrogen as a coolant it was possible to take measurements at three stable temperatures. When the nitrogen jacket was filled and the cryostat left to reach equilibrium the heat leak was such that the temperature at the sample was 150°K. When the helium space was filled with nitrogen the sample temperature was 77°K and by pumping on this nitrogen with an ordinary rotary pump a temperature of 65°K could be reached and maintained.

In the helium region only two temperatures were used. Measurements were made at 4.2°K in a liquid helium bath and at 1.4°K by pumping with a large capacity pump on the helium. The low temperature was measured from the vapour pressure of He^4 using a 0-20 torr absolute pressure guage. Intermediate temperatures could have been achieved by throttling the pump.

4.10. Magnet

The first magnet used was an electromagnet obtained from Mullard. This had 12 inch diameter polecaps and power was supplied

from a constant current power supply. At low temperatures the Zeeman relaxation time is generally of the order of hundreds of milleseconds so the time required to measure T_{1z} becomes relatively long. When this is combined with a sample with a narrow line the stability requirements of the magnet become quite severe. Using a simple proton magnetometer the drift of the 12 inch magnet was measured as being about 40×10^{-7} teslas per hour.

Although this was suitable for the samples with broad resonance lines the drift was too much for the narrow lines. For these samples a field regulated magnet with 9 inch diameter polecaps made by Varian was used.

4.11. Samples

4.11.1. Aluminium

Aluminium from two sources was used. The first was obtained from Reynold's Metal Company in the form of an atomised powder. This was quoted as being 99.99% pure and passed easily through a 300 mesh sieve. The second sample was prepared from a single crystal bar which had been repeatedly zone refined and had a resistance ratio of 3650. This was filed and passed through a 300 mesh sieve. It was then cleaned with a magnet to remove iron filings and annealed for one hour in an argon atmosphere at 360°C.

4.11.2. Copper

This was prepared from a copper rod of 99.99% purity by filing and passing through a 300 mesh sieve. It was then magnetically cleaned and annealed in an argon atmosphere for 30 minutes at 500°C.

Finally it was etched with weak hydrochloric acid, washed and vacuum dried.

4.11.3. Vanadium

Several samples were tried. The first was obtained in the form of a fine powder of 99.5% purity. Another sample was obtained from Johnson Matthey Chemicals in the form of large granules of 99.9% purity. This was filed, sieved, cleaned and annealed under ~0.1 torr of air for 1 hour at 1200°C. The third sample was obtained from the U.S. Bureau of Mines in the form of a small ingot of 99.99% purity. This was filed, sieved and cleaned and one half of the resultant powder was annealed for 1 hour at 1200°C under ~0.1 torr of air.

4.11.4. Cadmium

A very fine powder of 99.9999% pure cadmium was obtained from Metals Research Ltd., Cambridge.

4.11.5. Platinum

This metal was obtained from Johnson Matthey in the form of a chemical sponge. This passed easily through a 300 mesh sieve leaving only a few large lumps. The purity was 99.99%.

CHAPTER V - EXPERIMENTAL OPERATION

5. Experimental Operation

5.1. Measurement of T_{1z}

The Zeeman relaxation time was measured using a $90°-\tau-90°$[28,29] pulse sequence. It was not thought necessary to employ a pulse train[30] to saturate the magnetisation before applying the second pulse as the rotating r.f. field was intense enough to tip all the spins in the various samples. Because the conditions of exact phase, exact resonance and exact pulse width are not required to measure T_{1z} it was sufficient to set these conditions approximately by observing the signal on the oscilliscope. After a pulse the baseline has a slight time constant and returns slowly to the true zero position. To allow for this the height of the baseline without a signal, that is off resonance, must be noted, then the difference between this measurement and the measured signal height gives the true signal height. This is a very important correction for small signals.

Thus to measure T_{1z} the induction decay was found on the scope and adjusted for maximum using both phase and the width of both pulses. The relaxation time was then estimated from the behaviour of the signal after the second pulse as the separation of the pulses was varied. The repetition rate of the double pulse sequence was set at about $10T_{1z}$. The scope was triggered just before the first pulse and the timebase set for approximately $T_{1z}/5$ per division. With the field off resonance the zero was measured at each division on the scope and also at about $5T_{1z}$ after the first pulse.

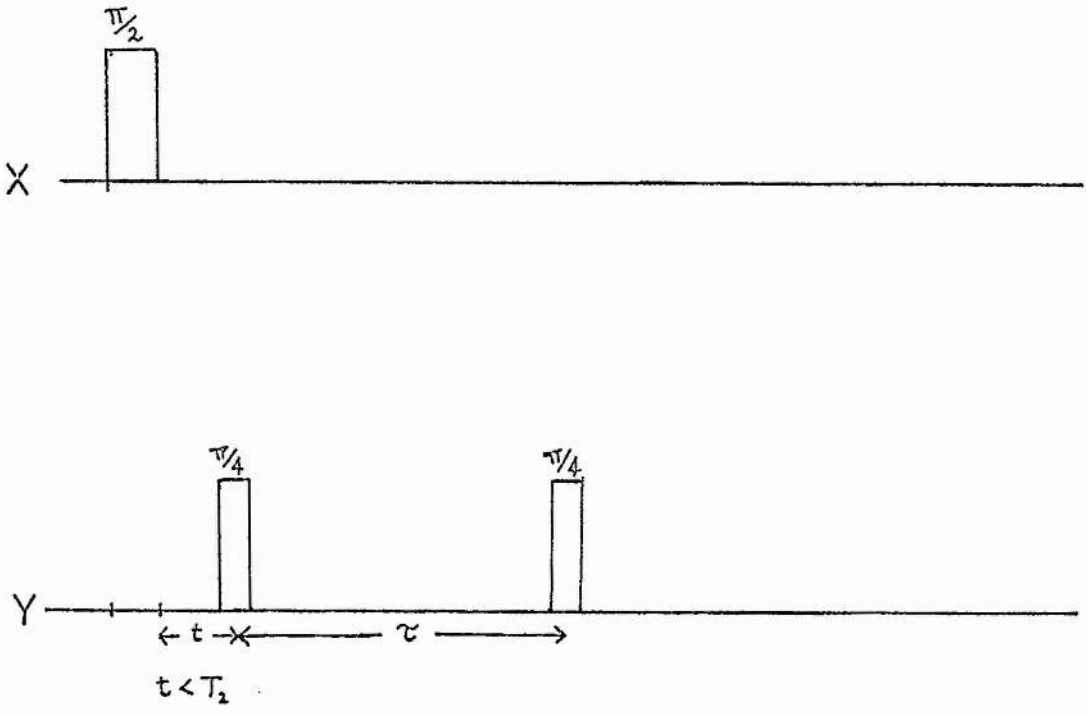

PULSE SEQUENCE FOR

MEASUREMENT OF T_{1eff}

Back on resonance the heights of the signal at these positions were measured and the true signal heights were calculated.

The measurement at $5T_{1z}$ gave the equilibrium magnetisation S_o. After the second pulse the signal is governed by

$$S(t) = S_o(1 - \alpha\, e^{-\frac{t}{T_{1z}}})$$

Thus

$$\frac{t}{T_{1z}} = \ln \alpha S_o - \ln(S_o - S(t))$$

By plotting $(S_o - S(t))$ against time on semi-log graph paper the relaxation time can be calculated directly from the slope of the resulting straight line. The factor α in the above equation allows for an error in phase or in the width of the first pulse. It can be seen that it has no effect on the measured relaxation time.

5.2. Measurement of T_{1dd}

To measure the dipolar relaxation time we must first convert order from the Zeeman to the dipolar energy bath. This requires a $\frac{\pi}{2}$ pulse followed by a $\frac{\pi}{4}$ pulse which is 90° phase shifted with respect to the first pulse. First the repetition rate is set for about $8T_{1z}$ and the $\frac{\pi}{2}$ pulse is set up by adjusting both pulse width and receiver phase for maximum signal as observed on the scope. The pulse width is then inspected by looking directly across the transmitter coil and the other pulses are made approximately $\frac{\pi}{4}$. After removing the $\frac{\pi}{2}$ pulse the signal after the $\frac{\pi}{4}$ pulses is adjusted for zero by varying both the field to be on exact resonance and the pulse phase to cancel the Zeeman signal. The $\frac{\pi}{2}$ pulse is switched back in and the dipolar signal after the

third pulse adjusted for maximum by varying the pulse widths and the separation of the $\frac{\pi}{2}$ and the first $\frac{\pi}{4}$ pulses. The third pulse is then moved to a time of about $4\ T_{1dd}$ after the pulse pair where the dipolar signal is negligible and the field and phase checked once more. The zeros are then taken with the field off resonance for each point to be measured. Back on resonance the phase of the third pulse is then finally adjusted to reproduce the zero reading thus ensuring that no Zeeman component is present. The signal heights are measured and by plotting these, corrected for zero error, against time on semi-log graph paper the dipolar relaxation time is obtained. The dipolar signal obeys the relation

$$S_{dd}(t) = S_{dd}(0)\ e^{-\frac{t}{T_{1dd}}}$$

After the signal heights are measured the third pulse is moved back to $4\ T_{1dd}$ to check that neither the field nor the phase has drifted. To minimise any slight drift the signal heights were usually measured from about $2\ T_{1dd}$ inwards towards the pulse pair as nearer the pulse pair the Zeeman signal is smallest and the dipolar signal largest so drift has very little effect.

5.3. Measurement of Second Moments

The values of δ obtained from some metals (Al and V) were sample dependent. Since the second moment is sensitive to defects and impurities in these metals[6] it was necessary to measure this property to acertain correctly the correlation between the values of δ and the purity of the samples.

It is possible using a pulse apparatus, a phase coherent receiver and a box-car integrator to obtain traces of the n.m.r. absorption signal[26] and hence the second moment[31]. The method requires that the box-car gate be set to cover the whole induction decay. Then by setting the receiver in phase or out of phase with the free precession and by sweeping the field at an appropriate rate the output from the box-car represents the absorption or the dispersion respectively. This method was used in an attempt to measure the second moment of aluminium. However the total decay time of the aluminium signal was of the order of 150μs and the dead time of the receiver was about 30μs after a pulse. Thus the signal was unobservable for the fifth of the total decay where the amplitude is largest. This was enough to render the above method unsuitable. The recordings obtained were not mixtures of absorption and dispersion but distorted versions of the correct signal. With the receiver in phase, for example, the trace obtained was a symmetric even function which looked like the absorption signal with bumps or beats added to the wings.

Second moments were eventually measured on a conventional c.ω. apparatus[31] using a crossed coil probe and a phase-shifter and attenuator[32] for decoupling.

5.4. Choice of Samples

The first measurements of dipolar relaxation times were performed on sodium, lithium, aluminium and copper[3,4]. Theory predicted that the values of $\delta = T_{1z}/T_{1dd}$ obtained should be

very close to 2. However the alkali metals gave $\delta = 2.2$, copper gave $\delta = 2.7$ and aluminium gave $\delta = 2.8$. The inclusion of many body effects into the theory partly explained the alkali metal results as a $\delta = 2.1$ was predicted[18]. The high values of δ in the other two metals could not be explained in this way.

The work described in this thesis was initiated by a desire to explain this discrepancy. It was deemed necessary to measure δ in other metals and over a wider temperature range than previous experiments. The metals studied were chosen for various different reasons.

Aluminium was initially chosen as a check on the reliability of the newly built apparatus because of its high sensitivity and availability of its n.m.r. parameters. However it proved to be interesting in its own light but similar metals were required before any conclusions could be drawn. Vanadium is very similar since it is cubic, has only one 100% abundant isotope, has a large quadrupole moment and very good sensitivity. Copper also fits this description except that it has two isotopes with nuclear moments. This however only slightly complicates the analysis of the results.

Cadmium and Platinum were chosen because both have spin $\frac{1}{2}$ and therefore no quadrupole moment, and because both have very large exchange interactions due to their high atomic numbers.

The experimental programme was thus to measure T_{1z} and T_{1dd} in these various metals over a wide range in temperature.

CHAPTER VI - ALUMINIUM

6.1. Results

The Zeeman relaxation time was measured in both samples at room temperature, taken as 295°K, and at 77°K. The values obtained were not sample dependent and led to a $T_{1z}T = 1.85 \pm .04$ sec°K, in excellent agreement with previous measurements.[3,4] The relaxation time at liquid helium temperatures was inferred from this result.

The dipolar relaxation time was measured over a wider range of temperature. The results obtained are summarised below

SAMPLE I	Temp	$T_{1z}/T_{1dd} = \delta$
99.99%	295°K	2.26 ± 0.03
	77°K	2.32 ± 0.05
	4.2°K	2.83 ± 0.04
SAMPLE II	295°K	2.25 ± 0.03
R.R. = 3650	77°K	2.47 ± 0.06
	65°K	2.54 ± 0.11
	4.2°K	2.92 ± 0.12
	1.4°K	2.87 ± 0.12

It is seen that the ratio is not constant but increases with decreasing temperature. At high temperatures δ is near the value of 2 predicted for pure dipolar relaxation and at low temperatures it approaches the value of 3 consistent with quadrupolar relaxation.

6.2. Discussion

Since $T_{1z}T$ is temperature independent the measured values of $T_{1dd}T$ show an explicit dependence on temperature. However if T_{1dd}

was purely the dipolar relaxation time δ could have no temperature dependence since it is the same mechanism relaxing the dipolar spins and the Zeeman spins. Thus the measured value of T_{1dd} must represent the true dipolar relaxation time plus a contribution from some other source. It is this extra contribution which produces the temperature dependence.

A clue to the origin of this extra contribution is obtained from the low temperature values of δ. The fact that this value is near 3 would imply that there was a large number of quadrupole spins taking part in the relaxation. It was first pointed out by Hebel[17] that in aluminium with a small concentration of impurities the zero field relaxation was due to two energy baths, one containing spins whose dominant interaction was dipolar and the other containing spins whose dominant interaction was quadrupolar. When these baths were cooled by adiabatic demagnetisation they first cross-relaxed via a temperature independent spin diffusion process to a common spin temperature and then relaxed together towards the lattice temperature. The second moment of our purest sample, II, was about 25% larger than the theoretical Van Vleck value showing that even in this case quadrupole interactions are important. The temperature dependence of δ can thus be explained by considering that the two energy baths become more and more decoupled as T_{1dd} becomes equal to and then much shorter than the temperature independent cross-relaxation time as the temperature increases. The influence of atomic diffusion on T_{1dd} can be neglected since this does not

contribute to the relaxation below about 240°C.[33]

The analysis of Jeener and Brockaert of the effects of a phase shifted pair of pulses applies only to transfer of order between Zeeman and dipolar energy baths. The expression they arrive at is a measure of the efficiency of this process. If only Zeeman and quadrupolar spin baths are considered, the quadrupole Hamiltonian being approximated by $\mathcal{H}_Q = -ahI_z^2$ in the rotating frame, the efficiency of transfer of order is zero provided $\gamma H_1 \gg a$.[82] In the cross-relaxation process envisaged above it is therefore assumed that immediately after the pulse pair the quadrupole spin bath is at the lattice temperature. Contact with the dipolar spins through cross-relaxation causes this temperature to deviate from its equilibrium position. Thus application of the third observation pulse might result in both dipolar and quadrupolar contributions to the signal. We can, however, neglect any quadrupole contribution because the time-independent term associated with quadrupole free induction decays[34] is zero and the oscillating terms will destructively interfere giving a net zero signal.

The approach to a common temperature of two spin systems coupled weakly to each other and to the lattice has been described mathematically by Schumacher.[35] Starting with two systems at different spin temperatures, $T_s^{(1)}$ and $T_s^{(2)}$, coupled to the lattice by mechanisms which produce relaxation rates R_1 and R_2, and exchanging energy with each other at rates R_{21} and R_{12}, the time dependence of the temperature of the two baths are given by

$$\frac{1}{T_s^{(1)}} = Ae^{m_+ t} + Be^{m_- t} + C$$

$$\frac{1}{T_s^{(2)}} = A'e^{m_+ t} + B'e^{m_- t} + C'$$

The constants A, B, C can be found from the initial conditions and A', B', C' are found by applying general rate equations to the system. The inverse time constants are given by

$$m_{\pm} = (1 + g + (1+\mu)h \pm s)$$

$$s = [(1-g)^2 + (1+\mu)^2 h^2 + 2h(\mu-1)(g-1)]^{\frac{1}{2}}$$

where $g = \frac{R_2}{R_1}$, $h = \frac{R_{12}}{R_1}$ and $\mu = \frac{R_{21}}{R_{12}}$ = ratio of heat capacities.

These equations have been applied to zero field relaxation in aluminium by Hebel[17], and by Fernelius[36] who measured a cross relaxation time of about 60 milliseconds in aluminium with 0.031 atomic percent of zinc impurity. The use of these equations with the value of 60 milliseconds for the cross-relaxation time and the low temperature (4.2°K) value of T_{1dd} leads to the conclusion that the heat capacity of the quadrupole bath is almost twice the heat capacity of the dipolar bath. Also the two time constants $\frac{1}{m_+}$ and $\frac{1}{m_-}$ should be very apparent but in fact the decay at 4.2°K was exponential within experimental error. With the values calculated for the low temperature results predictions can be made about the behaviour of the system at 77°K, the main one being that the measured δ should be about 2.7, still dominated by the quadrupole bath. This conflicts with the measured values in both samples.

The concept of two coupled energy baths, although explaining the measurements qualitatively, fails on closer examination to agree quantitatively. The main discrepancies are that the 4.2°K and the 77°K results cannot be explained by the same model, and a second component of the relaxation is predicted as being easily observable at 4.2°K but in fact was not observed. This second component was seen only at 1.4°K in sample II where it decayed in about 20 milliseconds and had a very small amplitude.

The requirements of a small quadrupole bath at 77°K and a large quadrupole bath at 4.2°K can be made compatible by considering three coupled energy baths. The results are all explained by a dipolar spin bath loosely coupled to a small quadrupole bath which is in turn even more loosely coupled to a large quadrupole bath, the cross-relaxation times being such that at 77°K only two baths are effectively coupled while at 4.2°K all three baths interact. That this is physically possible can be seen from the source of quadrupole interactions in a cubic metal such as aluminium. Around an impurity or a defect a large electric field gradient is formed by the screening action of the conduction electrons.[37] This field gradient has long range, it was found to affect about 100 spins around an isolated impurity[38], a large effect on neighbouring nuclei and a smaller effect on more distant nuclei. The nearest neighbours to an impurity are virtually isolated from all but their nearest neighbours because their energies are perturbed so much from the pure dipolar state. It was found by Minier et al[39] that about 78 neighbours had a quadrupole

interaction greater than 150 kHz and about 50 neighbours has interactions between 10 kHz and 100 kHz around a magnesium impurity.

The three bath system can be represented schematically thus:

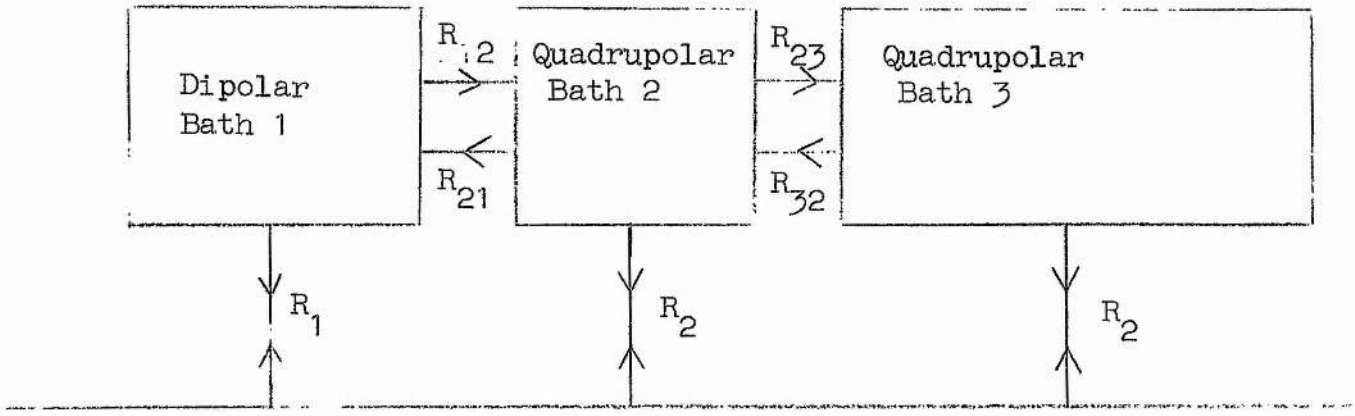

The rate of change of the spin temperatures of each bath can be written down by considering the above model

$$\frac{d}{dt}\left(\frac{1}{T_s(1)}\right) = -R_1\left(\frac{1}{T_s(1)} - \frac{1}{T_L}\right) - R_{12}\left(\frac{1}{T_s(1)} - \frac{1}{T_s(2)}\right)$$

$$\frac{d}{dt}\left(\frac{1}{T_s(2)}\right) = -R_2\left(\frac{1}{T_s(2)} - \frac{1}{T_L}\right) - R_{21}\left(\frac{1}{T_s(2)} - \frac{1}{T_s(1)}\right) - R_{23}\left(\frac{1}{T_s(2)} - \frac{1}{T_s(3)}\right)$$

$$\frac{d}{dt}\left(\frac{1}{T_s(3)}\right) = -R_2\left(\frac{1}{T_s(3)} - \frac{1}{T_L}\right) - R_{32}\left(\frac{1}{T_s(3)} - \frac{1}{T_s(3)}\right)$$

These coupled equations have the solution

$$\frac{1}{T_s(1)} = Ae^{m_1 t} + Be^{m_2 t} + Ce^{m_3 t} + D$$

$$\frac{1}{T_s(2)} = A'e^{m_1 t} + B'e^{m_2 t} + C'e^{m_3 t} + D'$$

$$\frac{1}{T_s(3)} = A''e^{m_1 t} + B''e^{m_2 t} + C''c^{m_3 t} + D''$$

where A, B, C, D are obtained from the initial conditions and the other constants are obtained from the rate equations. The three inverse time constants m_1, m_2 and m_3 are the three roots of the equation formed by substituting the solutions back into the rate equations and eliminating the constants A, A', A", etc. The resultant cubic is given by

$$m^3 + m^2R_1[1 + 2g + (1+\mu_{12})h_{12} + (1+\mu_{23})h_{23}] +$$

$$mR_1^2[g(2+g) + g(2+\mu_{12})h_{12} + g(2+\mu_{23})h_{23} +$$

$$(1+\mu_{23})h_{23} + \mu_{23}h_{23}(1+\mu_{12})h_{12} + \mu_{12}h_{12}] +$$

$$R_1^3[(1+h_{12})g^2 + (1+h_{12})(1+\mu_{23})h_{23}g + \mu_{12}h_{23}(g+\mu_{23}h_{23})] = 0$$

where $g = \frac{R_2}{R_1}$, $h_{12} = \frac{R_{12}}{R_1}$, $h_{23} = \frac{R_{23}}{R_1}$, $\mu_{12} = \frac{R_{21}}{R_{12}}$, $\mu_{23} = \frac{R_{32}}{R_{23}}$

This is solved by substituting numerical values and finding the roots.

The relaxation rate from the quadrupole baths to the lattice, R_2, is given by $3R_o$ where R_o is the Zeeman relaxation rate. To fit the equations to the results the dipolar relaxation rate, R_1, had to be $2.15\ R_o$. With a smaller value the results at 295°K and 77°K cannot be made compatible since the quadrupole bath required to explain the 295°K result would be too large to explain the 77°K result. A larger value of R_1 would imply almost no quadrupole effects at 295°K and too small a bath to explain the 77°K results. Thus in the above equations $g = 1.40$. The ratio of the heat capacities of bath 1 and bath 2 was found using a two bath model at 77°K, the best fit being obtained when $\mu_{12} = 2$. Use was made of

the fact that the cross-relaxation time between baths 1 and 2 was 20ms. The low temperature results were fitted using the three bath model with $\mu_{23} = 0.2$ and $R_{23} + R_{32} = 2$, that is a cross-relaxation time of 500ms.

Using these values to calculate the behaviour of the dipolar spin temperature at 1.4°K one obtains the equation

$$\frac{1}{T_s}(1) = Ae^{-1.265R_1t} + Be^{-1.790R_1t} + Ce^{-32.26R_1t}$$

The third component decays in a very short time and we are left with a situation similar to the two bath model since baths 1 and 2 have rapidly reached a common temperature and they are cross-relaxing to bath 3 as well as relaxing to the lattice temperature. Estimates can be made of the relative amplitudes of A and B. At 1.4°K A represents about 46% of the total amplitude so B must represent the other 54%. By adding the two exponentials and plotting them on semi-log graph paper over the range used to measure T_{1dd} a straight line is obtained, the slope of which gives a time constant between $\frac{1}{m_1}$ and $\frac{1}{m_2}$. Thus it seems that all measurements of T_{1dd} are obtained from an indistinguishable admixture of exponentials except at room temperature where only one component has a significant amplitude.

The values of δ obtained by fitting the theory of coupled spin baths to the experimental data are compared below to the measured values

Temp.	δ(calculated)		δ(measured)	
			sample I	sample II
1.4°K	3.00)	3-bath model		2.87
4.2°K	2.72)		2.83	2.92
65°K	2.52)	2-bath model		2.54
77°K	2.47)		2.32	2.47
295°K	2.23)		2.26	2.25

The agreement is very good at all temperatures for sample II but the 77°K value of δ for sample I seems rather low. This could be corrected by assuming either a smaller quadrupole bath 2 for this sample or a longer cross-relaxation time between baths 1 and 2. In view of the fact that the second moment of sample I was 14.6 $(\text{kHz})^2$ and the second moment of sample II was 12.3 $(\text{kHz})^2$ it seems unlikely that the quadrupolar bath of the more impure sample would be smaller so a longer cross-relaxation time which leaves the two baths almost uncoupled at 77°K seems the most reasonable explanation. A many bath model would perhaps be more correct physically but the mathematics of such a model would be formidable and the three bath model fits so well that further elaboration would be unjustified.

The temperature independent value of δ is thus 2.15. The error on this value consists of the error in the measurements and an error due to the approximate nature of the interpretation. The final conclusion is that for aluminium $\delta = 2.15 \pm .07$.

6.3. Evaluation of δ from Theory

The simple non-interacting electron theory 3,4 of nuclear spin-lattice relaxation in metals predicts a value of almost 2 for δ.

To explain a value of δ different from 2 use must be made of the theory due to Wolff[18] which takes account of electron-electron interactions. It was noted in section (3.3.2.) that before this theory could be applied some estimate of the strength of the electron-electron interaction must be found, that is a value must be given to α, the enhancement parameter. This parameter is related to the static electron spin susceptibility, χ_e, by the equation

$$\chi_e = \frac{\chi_o}{1-\alpha}$$

where χ_o is the calculated free electron susceptibility. However no measurements have been made of the spin susceptibility of aluminium so α must be evaluated by indirect methods.

The enhancement parameter appears in other expressions which describe processes affected by electron correlations. The theory of section (3.3.1.) showed that the Zeeman relaxation time, T_{1z}, is related to the Knight shift by the Korringa relation, equation (3.20). However the substitution of measured Knight shifts into this equation usually leads to a value of T_{1z} which is shorter than the measured relaxation time where, in fact, it should be longer to allow for the relaxation processes not allowed for in the theory. This discrepancy was corrected by Pines[16] who considered many body effects in the calculation of the spin suceptibility, leading to an enhanced Knight shift and hence to the modified Korringa relation of equation (3.21). It was pointed out by Moriya[41] that electron-electron interactions affect not only the Knight shift but also the spin-lattice relaxation time. This lead to a further modification

of the Korringa relation, the new expression being

$$T_{1z}T(\frac{\Delta H}{H})^2 = A(K(\alpha))^{-1} \qquad 6.1$$

where

$$A = \frac{\hbar}{4\pi k_B}(\frac{\gamma_e}{\gamma_n})^2$$

and

$$K(\alpha) = 2\int_0^1 \frac{(1-\alpha)^2 q\, dq}{[1-\alpha\, f(q)]^2} \qquad \text{with } q = Q/2k_F$$

The α and $f(q)$ are the same terms which appear in equation (3.23) derived by Wolff. Thus a knowledge of T_{1z} and $\Delta H/H$ should lead to an estimate of α using the above formulae. However this is only valid if the Knight shift and relaxation processes are dominated by the hyperfine contact interaction as this is the only process considered in the above theory.

The value of $T_{1z}T$ measured during the course of the research was $1.85 \pm .05$ sec °K. The Knight shift has been measured by Masuda and Redfield[42] who arrived at a value of $\Delta H/H = 0.162\%$. Thus in the Korringa relation $T_{1z}T(\Delta H/H)^2 = 1.26A$. Other relaxation processes and resonance shifts must be separated from those due to the contact interaction before the true value of $K(\alpha)$ can be found.

Electrons with s-wave character contribute to the Knight shift and the relaxation not only through the direct contact interaction but also through the core-polarization interaction. Because these effects cannot be distinguished experimentally the s-core polarization correction appears as a scale factor. The modified Korringa relation

becomes

$$(T_{1z}T_{c+cps})(\triangle H/H_{c+cps})^2 = A$$

The enhancement due to electron-electron interactions is unaffected.

The contributions to T_{1z} and $\triangle H/H$ from core-polarization due to the p-wave electrons cannot be treated in the above fashion. No cross terms exist between s-wave and p-wave electrons in a calculation of T_{1z} so the total relaxation rate $1/T_1$ is the sum of the individual rates each of which is related to the associated Knight shifts by a Korringa type relation. Thus contributions from this source must be subtracted before the effects of enhancement can be calculated. Calculations by Shyu, Das and Gaspari[43] show that the total contribution from the p-wave part of the electron wave function in aluminium to the Knight shift is negligible so contributions to the Korringa relation can be neglected.

The measured Knight shift could contain a contribution from the orbital motion of the conduction electrons. However there is some theoretical and experimental evidence that in aluminium this is negligible. A theoretical estimate of the shift due to an orbital interaction in aluminium was made by Appel[44] who put an upper limit on the orbital shift of 9% of the contact shift. In a superconductor the spin paramagnetism of the electron gas goes to zero as the temperature approaches zero so the Knight shift should also go to zero unless there is an orbital interaction present. It has been verified by Hammond and Kelly[45] to within the limits of their experiment that the Knight shift in aluminium does indeed go to zero. Thus it

seems justifiable to neglect any contributions to T_{1z} and $\Delta H/H$ from this source.

Because of the cubic symmetry of aluminium the dipolar interaction cannot act as a frequency shift mechanism but it can give a contribution to the relaxation rate. An estimate of this contribution can be made by applying the calculations of Obata[46]. Using the free electron density of states, assuming all conduction electrons to be in a p-band and estimating $\langle 1/r^3 \rangle$ from the known hyperfine splittings $a_{\frac{1}{2}}$ and $a_{3/2}$ in atomic aluminium, the resultant rate is of the order of 0.4% of the observed rate. These assumptions lead to an overestimate so relaxation due to electron-nucleus dipolar interactions can be neglected. It has been shown by Mitchell[47] that relaxation via the quadrupole interaction should be much less effective than relaxation via the dipolar interaction in the case of aluminium so this can also be neglected.

Thus there are no corrections to be made to the Korringa relation obtained from the measured values so $(K(\alpha))^{-1} = 1.26$. This leads to a value of $\alpha=0.38$ from the table of $K(\alpha)$ against α published by Narath and Weaver[48] who corrected the work of Moriya[41]. Like the theory of Wolff on the effect of electron correlations on δ, the theory of Moriya is only valid for simple metals whose Fermi surface is almost spherical and is wholly contained in the first Brillouin zone. The value of α determined above for aluminium can therefore have only qualitative significance.

By substituting this value of α and the values of k_F which provide the main contribution to the Knight shift[43] into equation (3.23) a value of δ corrected for electron-electron interactions is found. This value is $\delta = 2.06$. Thus the contribution to δ from electron correlations as calculated from the theory is a factor of two less than the measured value. This discrepancy could be due to the fact that the band structure and Fermi surface of aluminium are very different from the requirements of the theory or it could be due to a more fundamental limitation of the theory. This could be resolved by applying the theory to a simple metal where the assumption of a spherical Fermi surface is better met.

6.4. Evaluation of δ in Sodium

A careful study of the effects of electron-electron interactions on the Korringa relation in the alkali metals has recently been made by Narath and Weaver[48]. Among other metals, they studied sodium which is a good metal to use for testing the existing theories because not only is the Fermi surface almost spherical but a direct measurement has been made of α[49].

The substitution of the measured value of $\alpha = 0.42$ and the effective k_F of sodium into equation (3.23) and equation (6.1) leads to predicted values for δ and for the enhancement of the Korringa relation respectively. These are compared to the measured values in the following table:-

	Theory	Experiment
δ	2.03	2.12 ± 0.03[a]
$\frac{T_{1z}T(\Delta H/H)^2}{A}$	1.29	1.60 ± 0.07[b]

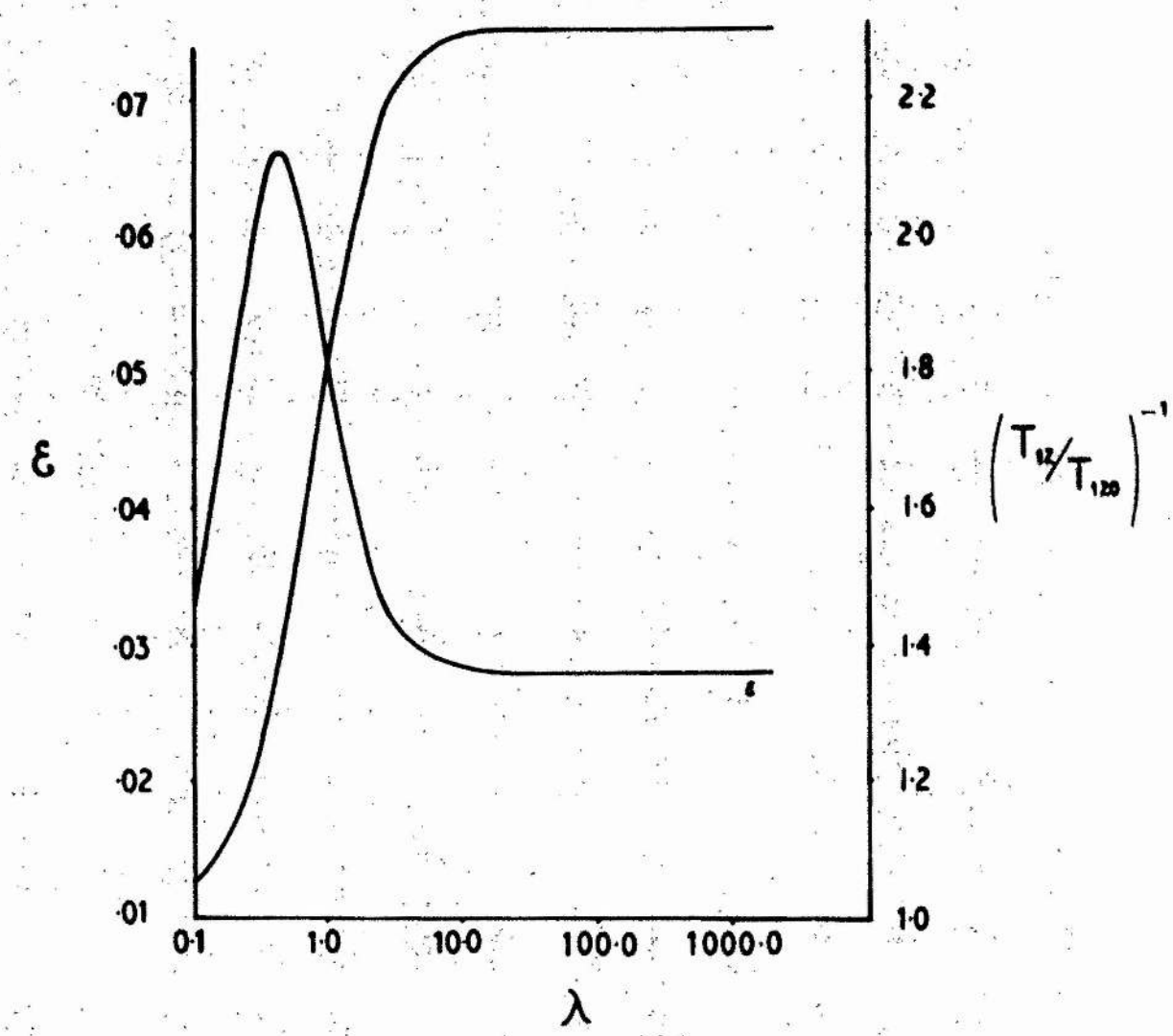
·07
·06
·05
·04
·03
·02
·01
ε
2·2
2·0
1·8
1·6
1·4
1·2
1·0
$\left(T_{12}/T_{120}\right)^{-1}$
0·1
1·0
10·0
100·0
1000·0
λ

FIGURE 9

a reference 50,51, b reference 48

It can be seen that in both cases the predicted effects of electron correlations are less than the measured effects.

Since the assumption of plane waves for the electron wave functions holds good for sodium it seems likely that the other assumption of the theories is at fault and that a delta-function interaction is not a proper description of the real interaction. However, as is pointed out by Narath and Weaver[48], the theory is only applicable when a delta-function interaction is used. Bearing this in mind they postulate a finite range for the interaction, assuming a potential of screened Coulomb form, in an effort to gain better agreement with the measured value of the Korringa enhancement. We have extended this analysis to the theory of Wolff in the hope that the improvement in the theoretical value of $T_{1z}T(\Delta H/H)^2/A$ would be duplicated for δ.

If the electron-electron interactions are of

(a) screened Coulomb type, then $\alpha = \alpha(0)[1+(q/\lambda)^2]^{-1}$

(b) Gaussian type, then $\alpha = \alpha(0)\exp[-q^2/4\beta^2]$

where q is the wave-vector difference between the interacting electrons. With these values of α in equation (3.23) numerical integration leads to curves of ϵ against λ and ϵ against β. Similar numerical integration of the demoninator of equation (3.23) gives curves for the enhancement of the Zeeman relaxation time against λ and β. Because both interactions produce similar curves only the screened Coulomb case is shown in figure 9; λ is in units of $2k_F$. When $\lambda = \infty$

in interaction (a) this corresponds to the delta-function interaction so the values for large λ obtained from figure 9 should correspond to the values quoted above. Since the enhancement of $(\Delta H/H)^2$ is determined by $\alpha(0)$ it is independent of λ. The value of T_{1z0}/T_{1z} for large λ is 2.3, which corresponds to a Korringa enhancement of 1.29, and the value of $\epsilon = 0.03$. Agreement with the experimentally observed Korringa enhancement is obtained when $\lambda = (1.0)2k_F$ which makes $\epsilon = 0.05$. Best agreement between theory and experiment for δ is obtained for $\lambda = (0.42)2k_F$ where $\epsilon = 0.07$, but the Korringa enhancement is then 2.23. The same difficulty is encountered with the gaussian interaction. Thus the assumption of a finite range for the electron-electron interaction improves the agreement between theory and experiment but the agreement is still unsatisfactory in the case of δ.

6.5. Summary

It has been shown that the return to equilibrium of the dipolar energy bath in aluminium is governed by contact with more energy baths than just the lattice. By taking account of these other energy baths the dipolar relaxation time to the lattice has been evaluated. The ratio of the Zeeman relaxation time to the dipolar relaxation time, δ, is 2.15 ± 0.07. A theoretical estimate of δ is given based on theories which take account of electron-electron interactions. The applicability of these theories, and modifications of these theories, is discussed in the case of a simpler metal sodium.

CHAPTER VII - COPPER

7.1 Results

The Zeeman relaxation times were measured for both isotopes of copper at 77°K. The value obtained for Cu^{63} was 15.6 ± 0.2 milleseconds leading to $T_{1z}T = 1.20 \pm 0.06$ sec °K. The value obtained for Cu^{65} was 13.97 ± 0.15 milliseconds. The ratio of the two relaxation times agrees, within error, with the square of the ratio of the gyromagnetic ratios of the two isotopes as predicted by equation (3.17).

The dipolar relaxation times were measured at 295°K and 77°K for both isotopes and at 4.2°K for Cu^{63}. At room temperature different values were obtained for each isotope, these values being

$$T_{1dd}^{Cu^{63}} = 1.67 \pm 0.06 \text{ ms} \qquad \delta = 2.43 \pm 0.14$$

$$T_{1dd}^{Cu^{65}} = 1.29 \pm 0.06 \text{ ms} \qquad \delta = 2.82 \pm 0.20$$

The same relaxation time, within error, was measured for both isotopes at 77°K.

$$T_{1dd}^{Cu^{63}} = 7.19 \pm 0.20 \text{ ms}$$

$$T_{1dd}^{Cu^{65}} = 6.83 \pm 0.28 \text{ ms}$$

When dipolar order is put into one spin system rapid flip-flops of the spins should lead to this order being shared with the other spin system in a time of the order of T_2. The two systems should then relax as one. Assuming that the relaxation time is the same for both isotopes, the average of all the 77°K values is $T_{1dd} = 6.97 \pm .10$ ms leading to values of δ of :

$$Cu^{63} \qquad \delta = 2.24 \pm .12$$

$$Cu^{65} \qquad \delta = 2.00 \pm .10$$

The low temperature measurement gave a value of $T_{1dd}^{Cu^{63}} = 104 \pm 6$ ms leading to $\delta = 2.75 \pm 0.30$ ms.

7.2. Discussion

The analysis of these results is complicated by the presence of two isotopes. It has been shown by Johnson and Goldburg[52] that when two spin species, x and y say, are present the dipolar relaxation from the energy bath represented by $\mathcal{H}_{dd} = \mathcal{H}_x + \mathcal{H}_y + \mathcal{H}_{xy}$ can be expressed in terms of the relaxation of the x spins and y spins separately. They find that

$$\frac{1}{T_{1dd}^{xy}} = \frac{\lambda}{T_{1dd}^{x}} + \frac{(1-\lambda)}{T_{1dd}^{y}}$$

where

$$\lambda = \frac{\mathrm{Tr}(\mathcal{H}_x^2)}{\mathrm{Tr}(\mathcal{H}_{dd}^2)} + \frac{1}{2}\frac{\mathrm{Tr}(\mathcal{H}_{xy}^2)}{\mathrm{Tr}(\mathcal{H}_{dd}^2)}$$

Substituting the relevent values for copper leads to

$$\frac{1}{T_{1dd}} = \frac{0.58}{T_{1dd}^{63}} + \frac{0.42}{T_{1dd}^{65}}$$

Assuming that δ is the same for both isotopes we can multiply the above equation by T_{1z}^{63} to get

$$\frac{T_{1z}^{63}}{T_{1dd}} = 0.58\,\frac{T_{1z}^{63}}{T_{1dd}^{63}} + 0.42\,\frac{T_{1z}^{65}}{T_{1dd}^{65}} \cdot \frac{T_{1z}^{63}}{T_{1z}^{65}}$$

$$= 0.58\,\delta + 0.42 \times 1.15 \times$$

$$= 1.06\,\delta \qquad 7.1$$

The measured values of $(T_{1dd}T)$ show the same temperature dependence as in aluminium. Since both copper isotopes have spin 3/2 and therefore quadrupole moments it is justifiable to assume that

the dipolar relaxation in this case is also modified by the presence of a quadrupole energy bath. Thus a temperature independent value of T_{1z}^{63}/T_{1dd} must be deduced from the measured values and then the correction of equation (7.1) applied to find the value of δ . Using the two bath model of Schumacher[35] the following model gave the best fit:

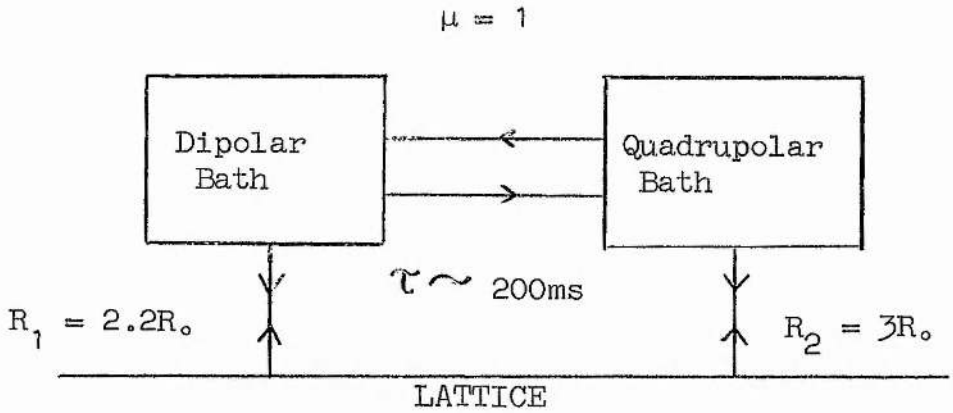

A larger value of R_1 would imply either a long cross-relaxation time or a small value of μ, the ratio of the heat capacities in order that the dipolar relaxation is not influenced by the quadrupole bath at 77°K. Both implications are incompatible with the low temperature result. A smaller value of R_1 would imply either that the cross-relaxation time was small or that μ was large so that the 77°K value could be increased by the presence of the quadrupole bath. Again this is not compatible with the low temperature value since this is explained by a cross-relaxation time comparable to R_1 and similar heat capacities for each bath since neither is dominant.

Thus we have a cross-relaxation time which is ten times longer than the direct cross-relaxation time in aluminium and a quadrupole bath which is similar in heat capacity. It has been shown by Rowland[53]

that the number of spins around an impurity in copper which have a quadrupole splitting greater than their dipolar splitting is smaller than in aluminium. Redfield[54] has shown that the quadrupole splittings in copper are greater than in aluminium. The low number of spins and the large difference in energies makes the spin-diffusion process of cross-relaxation inefficient so a large τ is understandable. However a small number of spins each with a large amount of quadrupole energy would have a similar heat capacity to a large number of spins each with a small amount of energy.

The two-bath model with the above parameters leads to the predictions

Temp.	T_{1z}^{63}/T_{1dd}(calc.)	T_{1z}^{63}/T_{1dd}(exp.)
77°K	2.24	2.24
4.2°K	2.82	2.75

The fit is good enought to accept that the temperature independent value of $T_{1z}^{63}/T_{1dd} = 2.20 \pm .15$. Substituting this value into equation (7.1) gives the value of δ in copper as $2.08 \pm .15$.

The room temperature measurements are unexplained by the above model. The fact that the dipolar relaxation times are different for the two isotopes would seem to indicate that internal equilibrium is not being reached in the dipolar system. The time between the pulse pair transferring order and the third observation pulse varied between 0.4 mS, which is only 2 T_2, and 2 mS so it appears likely that a state of true dipolar order was not being achieved. It must be noted however that the signal obeyed an exponential time dependence which one would not expect if the system were both

alligning to dipolar order and relaxing to the lattice at the same time. Jeener and Brockaert[23] state that in a single crystal of CaF_2 just after the pulse pair the observed signal changed in a rapid and complicated way until about $7T_2$ when the behaviour could be accounted for by means of spin-lattice relaxation alone. Flynn and Seymour[55] have shown that the onset of motional narrowing occurs in copper at about 800°C so it is unlikely that atomic motion would affect T_{1dd} at room temperature.

7.3 Evaluation of δ From Theory

No direct measurement has been made of the electron spin susceptibility in copper so a direct evaluation of α, the enhancement parameter is not possible. As before α can be deduced from the departure of the Korringa relation from the free electron model. Since copper is monovalent the Fermi surface almost fits the assumptions made in the theory of the effects of electron interactions. However the Fermi surface makes contact with the boundary of the first Brillouin zone so there is a large non-s character to the electron wave function. This must lead to some effects due to core-polarization, orbital interaction and dipolar interaction but these effects are not easily evaluated. Although it seems probable that some allowance should be made for contributions other than the contact interaction in the Korringa relation the neglect of these other effects will put an upper limit on the value of α and hence an upper limit on δ.

Narath and Weaver[48] have evaluated α using Moriya's theory[41] and previously published values of T_{1z} and $(\Delta H/H)$. They find

that for Cu^{63} $\alpha = 0.68$. By substituting this value into the theory due to Wolff a value of δ of 2.07 is obtained. Although this appears to be in remarkable agreement with the experimental value it must be noted that this represents an upper limit. A theoretical evaluation of the enhanced spin susceptibility of copper by Pines[16] gives a value of α of only 0.24 which would represent a δ of only 2.02.

7.4 Summary

The dipolar relaxation time has been measured for the 70% abundant Cu^{63} spins. After separating the effects of a coupled quadrupole bath and of the 30% abundant Cu^{65} spins a value of $\delta = 2.08 \pm .15$ has been obtained. This is in quantitative agreement with the theoretical value.

FIGURE 10

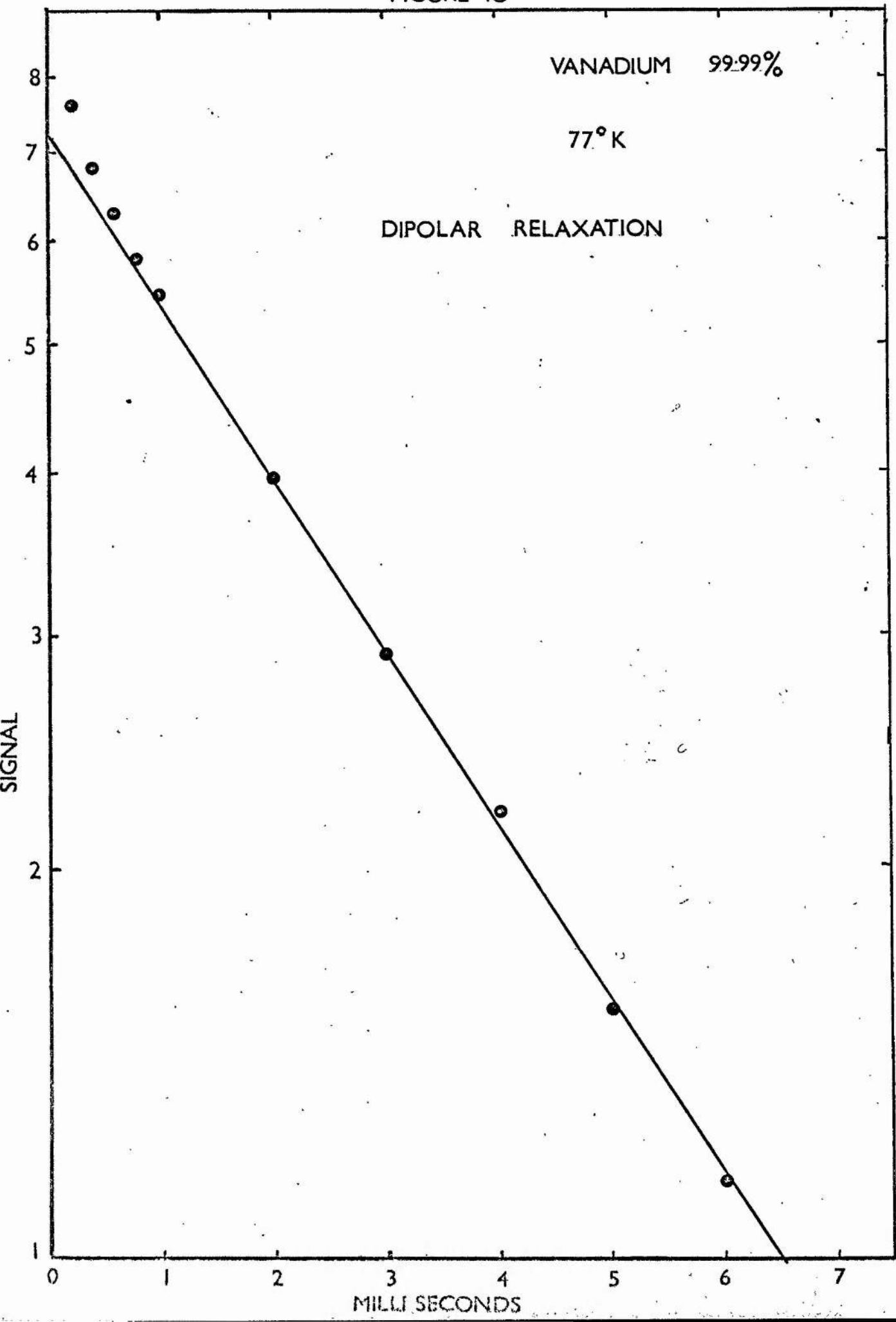
VANADIUM 99.99%
77° K
DIPOLAR RELAXATION
SIGNAL
8
7
6
5
4
3
2
1
0
1
2
3
4
5
6
7
MILLI SECONDS

CHAPTER VIII - VANADIUM

8.1. Results

The Zeeman and dipolar relaxation times were measured in three different samples. The results obtained are presented below.

	Sample	Temp	T_{1z}	T_{1dd}	δ
I	99.5%	295°K	2.75±.04ms	0.945±.014ms	2.90±.10
	Unannealed	77°K	9.18±.24ms	2.36±.14ms	3.88±.33
II	99.9%	295°K	Calc. from	0.72±.06ms	3.72±.40
	Annealed	77°K	$T_{1z}T=0.788 sec°K$[56]	0.81±.05ms	12.7 ±1.0
III	99.99%	295°K	2.75±.04ms	0.48±.03ms	5.74±.40
	Annealed				
	Unannealed	295°K	2.75±.04ms	1.16±.04ms	2.37±.14
		77°K	9.7 ± .6ms	3.36±.08ms	2.88±.24

It can be seen that the values of δ obtained are, in general, greater than those values obtained from copper and aluminium. Non-exponential decays were observed in the unannealed sample III. The value of T_{1dd} quoted is the time constant of the longest lived component though it was difficult to separate the two at room temperature since both time constants were off a similar time. A typical decay at 77°K is shown in figure 10. The short lived component was unobservable at both temperatures after about 0.8ms.

8.2. Discussion of Results

Vanadium has only one isotope with a nuclear magnetic moment. This isotope is 100% abundant ensuring good sensitivity and no complications from spin mixing. However the nuclei have spin

quantum number $I = 7/2$ and hence a large quadrupole moment so the presence of a quadrupole spin bath is to be expected.

The same trend as with the other metals in that δ increases with decreasing temperature is observed here. However there seems to be no correlation between low values of δ and high purity since sample II gives higher values than sample I although the former is purer, where as the unannealed sample of the purest metal gives, as before, the lowest values of δ . The pattern with vanadium is that unannealed samples give lower values of δ than annealed samples. This apparently conflicts with the theory that a large quadrupole bath leads to larger values of δ since the unannealed samples, containing more defects, should possess the larger quadrupole bath and so the larger values of δ .

The annealing of vanadium presents difficulties because the temperature of the metal must be high (melting point 1400°C) and at these temperatures the metal powder not only readily oxidises but also readily absorbs gases which can diffuse into the bulk. Sample II was annealed at 1200°C in air at about 0.1 torr for one hour and sample III was annealed at 1000°C in argon at about 0.1 torr for one hour.

The values of δ obtained from the unannealed purest sample most closely resemble the values obtained from the other metals. The same two bath model of a dipolar bath and quadrupolar bath can be used to explain these values. The 77°K result implies that there is a large quadrupole bath closely coupled to a smaller dipolar bath

since the value of δ is near 3. This then means that the temperature independent δ cannot be much greater than 2 or the room temperature value would be larger. Following the notation of Schumacher[35] the parameters required are $g = 1.40$, $\mu = 0.5$ and a cross relaxation time of about 3 ms. This means that the temperature independent value of $\delta = 2.15$. Although these parameters were chosen to give the best fit to the data the predicted value of δ at 295°K is larger than the measured value and the predicted value at 77°K is smaller than the measured value. Also the predicted amplitudes of the two components of the relaxation do not agree with the observed amplitudes. These are just the same problems met in the analysis of the dipolar relaxation in aluminium and, as in that case, better agreement could be obtained using a three bath model but the lack of data in vanadium excludes this. The temperature independent ratio of the Zeeman and dipolar relaxation times is then $\delta = 2.15 \pm .20$ where the error includes the measurement error and a contribution from the uncertainty in the analysis.

The two bath model can be used to explain qualitatively the high values of δ found in the other samples and the temperature independence of T_{1dd} in sample II. If the heat capacity of the quadrupole bath is much larger than that of the dipolar bath then the cross-relaxation will cause the temperature of the quadrupole bath to deviate very little from the lattice temperature. This means that when the dipolar spin lattice relaxation rate becomes small the cross-relaxation acts as a short-circuit and the temperature

independent cross-relaxation time is what one measures. A quadrupole bath with ten times the heat capacity of the dipolar bath and coupled to it with a cross-relaxation time of about 1 ms can be used to explain the values of δ in sample II as this leads to a value of $\delta \sim 4$ at 295°K and $\delta \sim 10$ at 77°K. It is possible since $T_{1dd} \simeq 4T_2$ that these values are distorted as was the case in copper.

The correlation between annealing and high values of δ can be understood by considering second moment measurements before and after the annealing. The calculated second moment for vanadium considering dipolar coupling alone is $24.2(\text{kHz})^2$ which can be compared to the value of $61 \pm 6(\text{kHz})^2$ for sample I, $55 \pm 5(\text{kHz})^2$ for sample III before annealing and $85 \pm 10(\text{kHz})^2$ for sample III after annealing. One would expect that after annealing the second moment would decrease as random defects in the crystal lattice have diffused out. These cause a reduction in the intensity of the absorption and add to the tails of the resonance[38], bath effects adding to the second moment. The fact that in this case it has increased must mean that during annealing impurities have diffused into the bulk of the sample. Other workers have reported a broadening of the vanadium resonance after annealing[57]. A vacuum of 10^{-8} torr was used by Redfield[58] to avoid contamination during the annealing of his vanadium samples. This was not possible in our case. Thus the same pattern as in aluminium of high values of δ being associated with low purity still holds with vanadium because the annealing process makes the metal very impure.

Although the presence of a large closely coupled quadrupole bath makes the analysis of dipolar relaxation times very imprecise a value of δ can be evaluated. Because the uncertainty in the value is large it is not clear if electron electron interactions are influencing the relaxation. The value of the ratio of Zeeman to dipolar relaxation times is $\delta = 2.15 \pm .20$.

8.3. Discussion of Theory

The Zeeman spin-lattice relaxation rate in vanadium contains contributions from the contact interaction, core polarization and the orbital interaction. The relative contribution from each source has been calculated theoretically by Yafet and Jaccarino[59]. They estimate that if the d-band in vanadium is equally represented by Γ_3 and Γ_5 orbitals then the orbital interaction is responsible for almost 60% of the observed relaxation rate. There is some experimental evidence to support this.[60,61] This mechanism should also dominate the dipolar relaxation rate. Such a mechanism is unaffected by electron spin correlations of the type discussed by Wolff[18] but spatial correlations are possible. In the case of no correlations and relaxation solely by the orbital interaction an estimate can be made of $\epsilon = \delta - 2$ using the theory of Obata[46]. The interaction Hamiltonian can be written as

$$\mathcal{H}_{orb} = \gamma_e \gamma_n \hbar^2 \frac{1}{r^3} \underline{I} \cdot \underline{l}$$

In the tight-binding approximation the Bloch wavefunctions are built up from localised atomic functions. These are chosen to

form the basis of irreducible representations of the cubic point group making the theory only applicable to cubic metals. From atomic functions, Φ_p, the Bloch functions, $\psi_{\mu\delta}(\underline{k},\underline{r})$, with eigenvalue $\mathcal{E}_{\mu\delta}(\underline{k})$ are constructed as follows:

$$\psi_{\mu\delta}(\underline{k},\underline{r}) = \sum_m U^p_{\mu\sigma}(k) N^{-\frac{1}{2}} \sum_R \exp(i\underline{k}.\underline{R}) \Phi_p(\underline{r}-\underline{R})\Theta$$

where μ is the band suffix, Θ_σ is the electron spin function, σ is the spin quantum number, $\underline{R}$ is the position vector of any atom in the crystal lattice, and N is the total number of atoms.

Approximating the nuclear plus electron wave functions as products of $\psi_{\mu\delta}(\underline{k},\underline{r})$ and the nuclear wave function, the transition probability per unit time of a nuclear spin transition between two nuclear states n and m, induced by the orbital interaction is given by

$$W_{mn} = \frac{2\pi}{\hbar}(\gamma_e\gamma_n\hbar^2)^2 \sum_{i,j}(n|\underline{I}_i|m)(m|\underline{I}_j|n)\ x$$

$$\sum_{\mu\sigma,\mu'\sigma'} \left\langle \mu k\sigma \left| \frac{1}{|\underline{r}-\underline{R}_i|^3}\underline{1} \right| \mu' k'\sigma' \right\rangle \left\langle \mu' k'\sigma' \left| \frac{1}{|\underline{r}-\underline{R}_j|^3}\underline{1} \right| \mu l\sigma \right\rangle x$$

$$\delta(\mathcal{E}_{\mu\sigma}(k) - \mathcal{E}_{\mu'\sigma'}(k') + \hbar\omega_I) f(\mathcal{E}_{\mu\sigma}(k))[1-f(\mathcal{E}_{\mu'\sigma'}(k'))]$$

By neglecting the Zeeman energy $\hbar\omega_I$, assuming that the temperature is much lower than the degeneracy temperature and summing over the atomic functions this reduces to

$$W_{mn} = \frac{2\pi}{\hbar}(\gamma_e\gamma_n\hbar^2)^2\ k_B T \rho^2(E_F) \sum_{ij}(n|\underline{I}_i|m)(m|\underline{I}_j|n)\ x$$

$$\sum_{pp'} C_p C_{p'} \left\langle \underline{mR}\,\sigma \left| \frac{1}{|\underline{r}-\underline{R}_i|^3} \right| \underline{m'R'}\sigma' \right\rangle \left\langle \underline{m'R'}\sigma' \left| \frac{1}{|\underline{r}-\underline{R}_j|^3} \right| \underline{mR}\,\sigma \right\rangle$$

where $\rho(E_F)$ is the density of electron states at the Fermi surface.

This transition probability is then substituted in the Hebel-Slichter formula, equation (3.16), to find the relaxation rate. It can be seen from W_{mn} that when $i = j$ the coefficient a_{ii} is given by

$$a_{ii} = \frac{2\pi}{\hbar} (\gamma_e \gamma_n \hbar^2)^2 k_B T \rho^2(E_F) \left\langle \frac{1}{r^3} \right\rangle^2$$

when $i \neq j$ the expectation value $\left\langle r^{-3} \right\rangle^2$ must be replaced by $\left\langle \frac{1}{(r-R_i)^3} \right\rangle \left\langle \frac{1}{(r-R_j)^3} \right\rangle$ which becomes, taking nucleus i as the origin $\left\langle \frac{1}{r^3} \right\rangle \left\langle \frac{1}{(r-R_{ij})^3} \right\rangle$. Because we are using the tight-binding approximation the expectation value $\left\langle \frac{1}{(r-R_{ij})^3} \right\rangle$ is a measure of the average distance of the wave function around nucleus i from the nucleus j. This can be approximated by R_{ij} since $r \ll R_{ij}$ so we then have

$$a_{ij} = \frac{R_{ij}^{-3}}{\left\langle r^{-3} \right\rangle} \; a_{ii}$$

This then gives an estimate of ϵ since $\delta = 2 + \frac{a_{ij}}{a_{ii}} = 2 + \epsilon$. The nearest neighbour distance for vanadium is 2.63Å. $\left\langle r^{-3} \right\rangle$ has been estimated[62] to be 1.35×10^{25} cm^{-3} for a 3d orbital round a vanadium ion and three-quarters of this value in the metal. This means that in the presence of correlations produced by electron wave function overlap only, $\epsilon = .005$.

8.4. Summary

The dipolar relaxation time has been measured for vanadium. The presence of a large quadrupole bath makes the evaluation of δ imprecise but a value of $\delta = 2.15 \pm .20$ has been inferred.

The effect of overlap of the electron wave function from one nuclear site to a neighbouring site has been evaluated. The large uncertainty in the value of δ masks the effects, if any, of spacial correlations from interacting electrons on the relaxation time. In the tight binding approximation the effect of spatial correlations from non-interacting electrons in vanadium is small; with reasonable approximations to the parameters involved, it seems unlikely that δ can be higher than 2.01. The contrast with the theoretical prediction for, say, aluminium, where $\epsilon = \delta - 2$, is several times larger, is caused by the different relaxation processes which are dominant in the two metals. Our experimental value is consistent with the theoretical analysis.

CHAPTER IX - PLATINUM

9.1. Results

The hyperfine fields at a nucleus increase with atomic number so it is expected that metals with high atomic numbers will have a large relaxation rate. This is the case with platinum (atomic no. 78) where at 77°K the Zeeman relaxation time is comparable to T_2. Thus measurements of T_{1dd} must be made in the liquid helium temperature range. The following results were obtained.

Temp.	T_{1z}	T_{1dd}	δ
4.2°K	7.32 ± 0.10ms	5.85 ± 0.15ms	1.25 ± 0.07
1.55°K	20.1 ± 0.2ms	15.4 ± 0.6ms	1.30 ± 0.07

The resonance line was inhomogeneously broadened as evidenced by the fact that a pulse sequence $\frac{\pi}{2} - \tau - \pi$ produced a spin echo at time 2τ.[28] This requires a magnetic field inhomogeneity across the sample in excess of the natural linewidth, a situation not common in solids. In this case the source of the inhomogeneity was not the magnetic field so a further source must be found to explain the echo formation.

9.2. Discussion of Results

The quoted purity of the platinum powder was 99.99% so it is unlikely that the observed inhomogeneity was caused by the presence of magnetic impurities. It was first pointed out by Drain[63] that magnetic resonance lines in solids could be broadened by macroscopic field inhomogeneities produced by the bulk magnetism of the sample. This must be taken into account in platinum which has both a narrow

line due to exchange narrowing and a high magnetic susceptibility. When seen under a microscope the metal powder consisted of different sizes of scales or discs which have large demagnetising factors. Random orientations of these scales could produce the observed inhomogeneity. The decay time of the observed induction decay was 250μs and the decay time of the echo envelope was about 1ms, in good agreement with previous measurements of T_2.[64,65] The short induction decay implies an inhomogeneity of about 4.4×10^{-4} teslas which is much larger than the value of 0.6×10^{-4} teslas predicted by Drain for randomly oriented spheroidal particles. However a disk would give a larger change in demagnetising factor with orientation than the particles he considers.

It must be pointed out that in the case of copper it was not possible to measure T_{1dd} satisfactorily when $T_{1dd} \sim 10T_2$. However in the case of platinum the value of δ obtained when $T_{1dd} \sim 6T_2$ agrees well with the value obtained when T_{1dd} is longer. It can only be assumed that it is the presence of the two isotopes in copper which leads to this discrepancy.

The three metals discussed in previous sections have all possessed quadrupole moments, a fact which has greatly complicated the analysis of δ. Platinum has only one isotope with a nuclear magnetic moment and spin $\frac{1}{2}$ and therefore no quadrupole moment. The natural linewidth of the platinum resonance is almost an order of magnitude narrower than that expected from dipolar broadening. This is attributed to exchange narrowing between like spins. The dipolar

interaction between nearest neighbours in platinum cannot exceed 130 Hz which is small compared to the strength of the exchange interaction of about 4kHz[66]. According to the theory of section (3.3.2.) this should lead to a value of δ less than two and indeed this is borne out by the measurements. We can write $\delta = 2 - 2\epsilon$ in the presence of a strong exchange interaction, where the measured value of ϵ for platinum is $\epsilon = 0.36 \pm .04$.

9.3. Discussion of Theory

Platinum, like vanadium, is a transition metal so the conduction electrons form an s-band and a d-band. This means that relaxation is caused not only by the contact interaction but also through the mechanisms of core polarization, and orbital and spin-dipolar interactions. An estimate of the relative importance of these interactions has been made by Yafet and Jaccarino[59]. In the case where the relative weights of Γ_3 and Γ_5 orbitals are equal they estimate that about 25% of the observed relaxation rate is due to core polarization, about 40% is due to the orbital interaction and about 35% is due to the contact interaction. Thus it is difficult to calculate a value of δ because the effects of interacting electrons is not known in the case where the relaxation is not solely via the contact interaction. Also the existing theory of these effects is strictly only applicable to simple metals with spherical Fermi surfaces. A qualitative value of δ can be calculated by naively neglecting these considerations. The measured electron spin susceptibility is a factor of two greater than the value calculated from low temperature specific heat measurements[64], which makes the enhancement parameter $\alpha = 0.5$. However the susceptibility,

proportional to the density of states of the electrons, calculated from specific heat measurements must be regarded as an upper limit since the density of states measured in this way is an enhanced value due to the electron - phonon interaction. Use of the 'bare' electron density of states would reduce the calculated susceptibility and hence increase α. Inserting $\alpha = 0.5$ and $k_F = 0.99 \times 10^8 cm^{-1}$, where k_F is the wave vector at the Fermi surface, into the theory of Wolff gives $\delta = 1.79$. This value would be reduced if α were larger but it seems unlikely that a value of $\delta = 1.28$ could be explained in this way. It is possible that electron interactions have more effect on the neglected relaxation processes than on the contact interaction but a more likely explanation of the discrepancy is the neglect of the structure of the Fermi surface.

9.4. Summary

The ratio of Zeeman to dipolar relaxation times has been measured in platinum. The value obtained, $\delta = 1.28 \pm .07$, is consistent with the presence of the dominant exchange interaction between nuclei. A calculated value, using a theory incorporating electron-electron interactions, is larger than the experimental value. This is thought to be due either to the Fermi surface of platinum being more complicated than simple Fermi surface assumed in the theory, or to the effects of electron correlations on dipolar relaxation caused by interactions other than the contact interaction.

CHAPTER X - CADMIUM

10.1. Results

At the onset of this work no measurements of the variation of the Zeeman relaxation time with temperature in cadmium had been reported in the literature so we undertook to measure T_{1z} in Cd^{113} over as wide a temperature range as possible. The values obtained are listed below with, for comparison, the values calculated from the Korringa relation using published Knight shifts.[67,68,69,70]

Temp.	T_{1z}(meas)	$T_{1z}T$(ms°K)	$(\Delta H/H)_{iso}$	$T_{1z}T$ (calc)(ms°K)
150°K	3.63±.36ms	545±60	0.36%	410
77°K	6.53±.23ms	507±20	0.35%	435
4.2°K	139 ± 7ms	588±20	0.34%	461
1.4°K	403 ± 20ms	565±20	0.34%	461

Cadmium has two isotopes with nuclear magnetic momensts, both only about 12% abundant. The resulting poor sensitivity meant that T_{1dd} could only be measured at helium temperatures. The two values for Cd^{113} obtained were:-

Temp.	T_{1dd}	δ
4.2°K	96 ± 6ms	1.45 ± .15
1.4°K	311 ± 20ms	1.30 ± .15

10.2. Discussion of Results

The Knight shift in cadmium shows an unusually large temperature dependence changing by 72% of its low temperature value between 4.2°K and the melting point. The small change of about 10% seen in other metals can usually be explained by a change in the lattice

parameters with temperature. This can be verified experimentally by reversing the expansion of the lattice with increasing temperature by applying pressure. However Kushida and Rimai[71] have shown from measurements of the pressure dependence of the Knight shift in cadmium that in this case the temperature dependence cannot be attributed to a change in the lattice parameters. It can be seen that the values of $T_{1z}T$ obtained experimentally are of the order of 20% longer than the values calculated by the Korringa relation and the temperature variation of $T_{1z}T$ closely parallels that of the Knight shift. An extension of our measurements up to and beyond the melting point has been carried out by Dickson[72] who found the same as above to hold over the whole range to the melting point. Above the melting point the measured and calculated values of $T_{1z}T$ differed by about 40%. The fact that an enhanced Korringa relation is obeyed over the whole temperature range implies that the temperature dependence is due to some variation of the electronic properties in cadmium.

A similar case of a large temperature dependence of the Knight shift and $T_{1z}T$ has been reported in the intermetallic compound $AuGa_2$[73]. This was explained by considering a change in the character of the Fermi surface. At low temperatures the electron-nucleus interaction was predominantly core-polarization due to a large component of p-type electron wave function at the Fermi surface. As the temperature was raised the s-type wave function became more predominant and the interaction was thus mainly the contact interaction. This model explained the variation of the Knight shift and $T_{1z}T$ with

temperature but due to the difficulty of constructing a sensible band structure the explanation remained phenomenological. Using the band structure of Stark and Falikov[74] for cadmium this same model has been applied[75] in a more rigorous manner to fully explain the temperature variation of the Knight shift in this metal. The effect was shown theoretically to be due to the temperature washing out of electronic structural effects to T=0°K, which are due to strong pseudopotentials.

The first measurement of T_{1z} in cadmium was made by Masuda[76] using a continuous wave technique[31]. He found that at room temperature $T_{1z}T = 150 ms°K$, much less than the value predicted by the Korringa relation, so other relaxation processes were used to explain the discrepancy. It has now been shown that this value is wrong[72] and at room temperature the value of $T_{1z}T$ is in excess of the predicted value. The importance of relaxation mechanisms other than the contact interaction can be estimated. At low temperatures cadmium has an s-band and a d-band. As the temperature is increased the importance of the d-band diminishes and the anisotropic Knight shift is explained by the interaction with p-type electrons. Therefore in considering other relaxation processes only s-type and p-type electrons will be considered. The use of d-type electrons would not affect the conclusions and would modify the details only slightly.

Obata[46] has calculated, for p-bands in cubic metals, the rate of relaxation to be expected from the dipolar and orbital interactions.

$$\left(\frac{1}{T_{1z}T}\right)_{dip+orb} = \frac{13\pi}{45\hbar}\left[\gamma_e\gamma_n\hbar^2 N(E_F)\left\langle r^{-3}\right\rangle\right]^2 k_B$$

To apply this equation to cadmium values of $N(E_F)$, the free electron total density of states at the Fermi surface, and $\left\langle r^{-3}\right\rangle$ are required. The density of states can be obtained from the low temperature specific heat data of Phillips[77] which leads to $N(E_F) = 18.2 \times 10^{10}$ erg^{-1} atom^{-1}. An estimate of $\left\langle r^{-3}\right\rangle$ can be made using the optical hyperfine splitting parameters, $a_{\frac{1}{2}}$ and $a_{3/2}$ of Lurio and Novick[78] and standard formulae quoted by Kopfermann[79]. The hyperfine splitting parameters are given by

$$a_j = a_{l\pm\frac{1}{2}} = a_{n,l}\frac{l(l+1)}{j(j+1)} F_r(j,Z)$$

where $$a_{nl} = \frac{\mu_o}{4\pi} 2\mu_B^2 \left\langle r^{-3}\right\rangle g_I$$

and $$F_r(j,Z) = \frac{4j(j+\frac{1}{2})(j+1)}{\rho(4\rho^2-1)}$$

with $$\rho = \sqrt{(j+\tfrac{1}{2})^2 - \alpha^2 Z^2}$$

Values of $\left\langle r^{-3}\right\rangle$ were calculated using $a_{\frac{1}{2}}$ and $a_{3/2}$ and the average value was $\left\langle r^{-3}\right\rangle = 3 \times 10^{25}$cm^{-3} in agreement with the value used by Masuda[76]. Inserting these values into Obata's formula gives $T_{1z}T = 20$sec°K, thus the neglect of these relaxation processes is justified.

The fact that the Knight shift shows a jump of 33% at the melting point is interpreted by Dickson[72] to mean that the core-polarization contribution has vanished. He estimated that in the solid $K_{cp}/K_{contact} \simeq -9\%$ where $K = (\Delta H/H)$. Yafet and Jaccarino[60] have

calculated the contribution to the relaxation rate due to core polarization. Compared to the relaxation rate due to the contact interaction we have

$$\frac{(1/T)_{cp}}{(1/T)_{contact}} = \frac{1}{3}\,(K_{cp}/K_{contact})^2$$

Thus $$\left(\frac{1}{T}\right)_{cp} \simeq \frac{1}{300}\left(\frac{1}{T}\right)_{contact}$$

in the case of cadmium, so this contribution can be neglected.

Thus the relaxation in cadmium is due mainly to the contact interaction whereas the Knight shift has a small contribution due to core-polarization. After allowing for this contribution a value of α can be deduced from the enhanced Korringa relation. Using the theory of Moriya[41] and interpolating the table of Narath and Weaver[48] a value of $\alpha = 0.52$ is obtained.

The density of states derived from specific heat measurements can also be used to calculate $\mathcal{E}$, the s-content of the electron wave function at the Fermi surface, by substituting in the Knight shift formula. This procedure requires independent values of the spin susceptibility and $\left\langle \left| U_k(0) \right|^2 \right\rangle_{EF}$. The susceptibility was calculated using $X_s = X_o(1-\alpha)^{-1}$ where $X_o = \mu_B^2\, N(E_F)$ and the $(1-\alpha)^{-1}$ factor allows for the enhancement due to many body effects. $\left|\Phi_s(0)\right|^2_A$ was obtained from the optical hyperfine parameter a_s[78]. We suppose that

$$\frac{\left\langle \left|\Phi_s(0)\right|^2 \right\rangle_{E_F}}{\left|\Phi_s(0)\right|^2_A} = 0.7$$

where $\left|\Phi_s(0)\right|^2_A$ is the probability density at the nucleus for a

5s electron in the free atom. The factor 0.7 allows for the expansion of the wave function in the metal. The s-content is introduced through

$$\left\langle \left| U_k(0) \right|^2 \right\rangle_{E_F} = \xi \left\langle \left| \Phi_s(0) \right|^2 \right\rangle_{E_F}$$

The measured values of the Knight shifts were adjusted by allowing for the core polarization contribution. The derived values were substituted in

$$\left(\frac{\Delta H}{H}\right)_{\text{contact}} = \frac{8\pi}{3} K \xi \left\langle \left| \Phi_s(0) \right|^2 \right\rangle_{E_F} \chi_s \Omega$$

where K is a relativistic correction (1.28 in this case), χ_s is in c.g.s. volume units and Ω is the atomic volume. This leads to $\xi = 0.242$ at 77°K and $\xi = 0.235$ at 4.2°K. This is in essential agreement with the band structure calculations of Stark and Falikov[74].

The second moment of cadmium at room temperature[76] is $0.53(\text{kHz})^2$ which is more than ten times the value for classical dipolar coupling which is $0.045(\text{kHz})^2$. The extra broadening is attributed to exchange broadening[11] or pseudo-dipolar broadening[10]. The large exchange interaction would lead one to predict a value of δ less than 2 provided some correlation was present, which is the case as can be seen from the non-zero value of α. Wolff's theory for δ should be more valid for cadmium because of the large contact interaction contribution to the relaxation. However a value of δ predicted in this way can still have only qualitative meaning as the Fermi surface does not meet the requirements of the theory. A value of $\delta = 1.90$ is obtained.

Cadmium has two isotopes with nuclear moments so before the experimental and theoretical results can be compared the measured value must be corrected in a similar manner to copper. The equation connecting the real and apparent values is:-

$$\frac{T_{1z}^{113}}{T_{1dd}} = \lambda \frac{T_{1z}^{113}}{T_{1dd}^{113}} + (1-\lambda) \frac{T_{1z}^{111}}{T_{1dd}^{111}} \cdot \frac{T_{1z}^{113}}{T_{1z}^{111}}$$

Because the two isotopes are similar in abundance and gyromagnetic ratio, and because the dominant contribution to the second moment is due to terms coupling unlike spins we will take $\lambda = 0.5$. Since $T_{1z}^{113}/T_{1z}^{111} = 0.91$ and $T_{1z}^{113}/T_{1dd} = 1.37$ we have $\delta = 1.43 \pm .15$.

10.3. Summary

The measured values of $T_{1z}T$ in cadmium are larger than the values predicted by the Korringa relation. This is attributed to electron-electron interactions and after separating from the Korringa product contributions from non-s-type electrons an estimate of the strength of these interactions is obtained by evaluating α, the enhancement parameter. Using this same parameter to calculate δ leads to a theoretical value greater than the measured value. Due to the relaxation being dominated by the contact interaction the unknown effects of correlations on other relaxation mechanisms cannot be invoked to explain this discrepancy. It appears that the departure of the Fermi surface in cadmium from that required by the theory must be the cause of the discrepancy between theoretical and experimental values of δ.

CHAPTER XI - SUMMARY

This thesis is a report of an experimental and theoretical investigation of dipolar spin-lattice relaxation times in pure metals. Both the usual Zeeman as well as the dipolar relaxation times were measured as a function of temperature in Al^{80}, Cu, V, Cd^{81} and Pt. The metals Al, Cu and V all have nuclear spin $> \frac{1}{2}$ so they show strong quadrupole effects which complicate the analysis. Non-exponential spin-lattice decays are observed in these metals. A model explaining this and leading to the elucidation of the true dipolar relaxation time is presented. These complications are not present for Cd and Pt since they both have nuclear spin $\frac{1}{2}$ and hence no quadrupole moment. In these metals however the dipolar relaxation is strongly influenced by the presence of indirect nuclear-nuclear couplings.

These measurements require the use of a phase-coherent pulse spectrometer capable of measuring spin-lattice relaxation times over a wide temperature range. A suitable apparatus and the experimental techniques are described.

The parameter discussed in the relevent theories of dipolar relaxation is δ, the ratio of Zeeman to dipolar relaxation times. The following values were found.

Al	$\delta = 2.15 \pm .07$
Cu	$\delta = 2.08 \pm .15$
V	$\delta = 2.15 \pm .20$
Pt	$\delta = 1.28 \pm .07$
Cd	$\delta = 1.43 \pm .15$

The overlap with previous investigations concerned the metals Al and Cu. The results reported here are in considerably better agreement with theory.

The general characteristic of the results is the need to invoke electron-electron interactions in an explanation of the values of δ. The measurements in Pt and V are difficult to interpret because their dominant relaxation mechanisms are not discussed in existing theories. A theory of nuclear relaxation which considers the effects of a delta-function interaction between electrons partially explains the remaining results but a residual discrepancy exists in all cases. This may be due to the restrictive assumptions of the theory which make it relevant only to simple metals. Of the metals investigated here Cu approaches the requirements most closely. However application of the theory to a simple metal such as Na still leaves a discrepancy between predicted and measured values of δ. The effects of introducing a finite range to the electron-electron interaction are discussed.

It appears that failure to fully explain the results is due in part to the inherent inadequacies of existing theories and in part to the complicated electronic structures of the metals investigated which make the formulation of a more general theory very difficult.

REFERENCES

1. F. Bloch, W.W. Hanson and M.E. Packard (1946) Phys. Rev. 69, 127.

2. E.M. Purcell, H.C. Torrey and R.V. Pound (1946) Phys. Rev. 69, 37.

3.(a) L.C. Hebel and C.P. Slichter (1959) Phys. Rev. 113, 1504.
3 (b) C.P. Slichter Principles of Magnetic Resonance
4. A.G. Anderson and A.G. Redfield (1959) Phys. Rev. 116, 583.

5. M.H. Cohen and F. Reif (1957) Solid State Phys. 5, 321.

6. N. Bloembergen and T.J. Rowland (1953) Acta. Met. 1, 731.

7. C.H. Townes, C. Herring and W.D. Knight (1950) Phys. Rev. 77, 853.

8. W.M. Shyu, T.P. Das and G.D. Gaspari (1966) Phys. Rev. 152, 270.

9. R.J. Noer and W.D. Knight (1964) Rev. Mod. Phys. 36, 177.

10. N. Bloembergen and T.J. Rowland (1955) Phys. Rev. 97, 1679.

11. M.A. Ruderman and C. Kittel (1954) Phys. Rev. 96, 99.

12. J.H. Van Vleck (1948) Phys. Rev. 74, 1168.

13. L.C. Hebel (1963) Solid State Phys. 15, 409.

14. C.J. Gorter (1940) Phys. Rev. 57, 426

15. J. Korringa (1950) Physica 16, 601.

16. D. Pines (1955) Solid State Phys. 1, 367.

17. L.C. Hebel (1962) Phys. Rev. 128, 21.

18. P.A. Wolff (1963) Phys. Rev. 129, 84.

19. J. Winter (1963) J. Physique 24, 1127.

20. A.G. Anderson and S.R. Hartmann (1962) Phys. Rev. 128, 2023.

21. B.C. Johnson and W.I. Goldburg (1966) Phys. Rev. 145, 380.

22. J. Poitrenaud and J.M. Winter (1965) Phys. Rev. Letters 17, 199.

23. J. Jeener and P. Brockaert (1967) Phys. Rev. 157, 232.

24. J. Jenner, H. Eisendrath and R. Van Steenwinkel (1964) Phys. Rev. 133, A478.

25. R.J. Blume (1961) Rev. Sci. Instr. 32, 554.

26. W.G. Clark (1964) Rev. Sci. Instr. 35, 316.

27. D.F. Holcomb and R.E. Norberg (1955) Phys. Rev. 98, 1074.

28. E.L. Hahn (1950) Phys. Rev. 80, 580.

29. H.Y. Carr and E.M. Purcell (1954) Phys. Rev. 94, 630.

30. A. Narath and D.W. Alderman (1966) Phys. Rev. 143, 328.

31. E.R. Andrew(1958) Nuclear Mangetic Resonance (Cambridge University Press).

32. R.J. Blume (1963) Rev. Sci. Instr. 33, 1472.

33. F.Y. Fradin and T.J. Rowland (1967) App. Phys. Letters 11, 207.

34. I. Solomon (1958) Phys. Rev. 110, 61.

35. R.T. Schumacher (1958) Phys. Rev. 112, 837.

36. N. Fernilius (1967) Magnetic Resonance and Relaxation ed. by R. Blinc (North-Holland Publishing Co.).

37. J. Friedel (1952) Phil. Mag. 43, 153 ; (1954).Advan. Phys. 3, 446 ; (1958) Nuovo Cimento Suppl. 2, 287.

38. T.J. Rowland (1955) Acta. Met. 3, 74.

39. M. Minier, J. Levin, P. Averbuch and D.P. Tunstall (1967) 4th Annual Solid State Phys. Conference.

40. Radio Amateurs Handbook 38th Ed. (1961).

41. T. Moriya (1963) J. Phys. Soc. Japan 18, 516.

42. Y. Masuda and A.G. Redfield (1964) Phys. Rev. 133, A944.

43. W.M. Shyu, T.P. Das and G.D. Gaspari (1966) Phys. Rev. 152, 270.

44. J. Appel (1965) Phys. Rev. 139, A1536.

45. R.H. Hammond and G.M. Kelly (1967) Phys. Rev. Letters 18, 156.

46. Y. Obata (1963) J. Phys. Soc. Japan 18, 1020.

47. A.H. Mitchell (1957) J. Chem. Phys. 26, 1714.

48. A. Narath and H.T. Weaver (1968) Phys. Rev. 175, 373.

49. R.T. Schumacher and W.E. Vehse (1963) J. Phys. Chem. Solids 24, 297.

50. D. Jerome and G. Gallerron (1963) J. Phys. Chem. Solids 24, 1557.

51. J. Poitrenaud and J.M. Winter (1965) Phys. Letters 17, 199.

52. B.C. Johnson and W.I. Goldburg (1966) Phys. Rev. 145, 380.

53. T.J. Rowland (1960) Phys. Rev. 119, 900.

54. A.G. Redfield (1963) Phys. Rev. 130, 589.

55. C.P. Flynn and E.F.W. Seymour (1961) Proc. Phys. Soc. 77, 922.

56. J. Butterworth (1960) Phys. Rev. Letters 5, 305.

57. L.E. Drain Private Communication.

58. W. Fite and A.G. Redfield (1967) Phys. Rev. 162, 358.

59. Y. Yafet and V. Jaccarino (1964) Phys. Rev. 133, A1630.

60. J. Butterworth (1964) Proc. Phys. Soc. 83, 71.

61. R.J. Noer and W.D. Knight (1964) Rev. Mod. Phys. 36, 177.

62. A.M. Clogston, A.C. Gossard, V. Jaccarino and Y. Yafet (1962) Phys. Rev. Letters 9, 262.

63. L.E. Drain (1962) Proc. Phys. Soc. 80, 1380.

64. A.M. Clogston, V. Jaccarino and Y. Yafet (1964) Phys. Rev. 134, A650.

65. R.E. Walstedt, M.W. Dowley, E.L. Hahn and C. Froidevaux (1962) Phys. Rev. Letters 8, 406.

66. C. Froidevaux and M. Weger (1964) Phys. Rev. Letters 12, 123.

67. E.F.W. Seymour and G.A. Styles (1964) Phys. Letters 10, 269.

68. R. Borsa and R.G. Barnes (1966) J. Phys. Chem. Solids 27, 567.

69. H.E Schone (1964) Phys. Rev. Letters 13, 12.

70. S.N. Sharma and D.L. Williams (1967) Phys. Letters 25A, 738.

71. T. Kushida and L. Rimai (1966) Phys. Rev. 143, 157.

72. E.M. Dickson Thesis, University of California (unpublished), (1969) Phys. Rev. 184, 294.

73. V. Jaccarino, M. Weger, J.H. Wernick and A. Menth (1968) Phys. Rev. Letters 21, 1811.

74. R.W. Stark and L.M. Falikov (1967) Phys. Rev. Letters 19, 795.

75. R.V. Kasowski and L.M. Falikov (1969) Phys. Rev. Letters 22, 1001.

76. Y. Masuda (1957) J. Phys. Soc. Japan 12, 523.

77. N.E. Phillips (1964) Phys. Rev. 134, 385.

78. A. Lurio and R. Novick (1964) Phys. Rev. 134, A608.

79. H. Kopfermann (1958) Nuclear Moments (Academic Press).

80. D.P. Tunstall and D. Brown (1968) Phys. Letters 27A, 723.

81. D.P. Tunstall and D. Brown (1968) Phys. Letters 28A, 445.

82. D.P. Tunstall (Private Communication)